Physical and biogeochemical variability in the Gulf of La Spezia (Eastern Ligurian Sea, Italy): insights from new high-resolution coastal observatory

Tiziana Ciuffardi[1], Silvia Becagli[2], Giancarlo Raiteri[1], Andrea Bordone[1], Erica Gabrielli[1,3], Marcello G. Magaldi[4], Andrea Peirano[1], Fabio Piccolin[1], Petrika Gjanci[5], Chiara Petrioli[5,7], Daniele Spaccini[5], Marinella Abbate[1], Ivo Rossetti[1], Paolo Varrella[6], Chiara Lombardi[1*]

[1] Marine Environment Research Centre S. Teresa ENEA, Lerici (SP), 19032, Italy

[2] Department of Chemistry 'U. Schiff', University of Florence, Sesto Fiorentino (FI), 50019, Italy
[3] Department of Earth and Environmental Sciences, University of Milano Bicocca, Milano, 20126, Italy
[4] Institute of Marine Sciences, CNR, Lerici (SP), 19032, Italy
[5] W•SENSE S.r.l., Rome, 00198, Italy
[6] Cooperativa Mitilicoltori Associati, Lerici (SP), 19032, Italy
[7] Computer Engineering Department, University of Rome La Sapienza

Corresponding author: Chiara Lombardi (chiara.lombardi@enea.it)

Abstract

Coastal marine shallow sites, characterised by biological richness and diversity, experience fluctuations in seawater physical and chemical variables. However, given the complexity of coastal processes and dynamics, exacerbated by the climate change effects, it is becoming hard to predict the fate of marine systems.

High-resolution observatories enable big data acquisition through continuous monitoring, improve the real-time detection of oceanic changes, especially at local scale, and provide essential data for marine system predictions and early warning capabilities for maritime activities. However, comprehensive long-term, high-resolution datasets in coastal areas are still limited.

Smart Bay Santa Teresa underwater observatory, a new high-resolution system located in the Eastern Ligurian Sea, provided physical and biogeochemical data continuously from 2021 to 2024. Physical data confirmed a warming trend of 0.045 °C per year in the study area, consistent with global climate change patterns, and increased frequency and intensity of Marine Heatwaves, especially in 2022-2023. Biogeochemical data revealed an enriched carbonate environment, despite the short-term perturbations, and a shift of biogenic and thermal control of the carbonate system through seasons favoring biogenic carbonate development (i.e. mussels' reefs). Interestingly, the balance between CO_2 stock and release, derived from biogenic calcification, revealed that the area as an active carbon sink, especially in winter and spring.

The ecological value and biodiversity of the coastal marine ecosystems coexisting with highly anthropogenic areas make the site ideal to monitor the interacting effects of global warming, local hydrodynamics, and seasonal biogeochemical processes through integrated monitoring approaches.

Keywords 1-7
marine observation, Mediterranean Sea, coastal site, Internet of Underwater Things, marine carbonate system, marine ecosystems

Highlights

1. A warming trend of 0.045 °C per year in the area with long-term temperature records.
2. Increased frequency and intensity of Marine Heatwaves (MHWs) (2022-2023)
3. Altered local hydrodynamic regime due to the dam.
4. Enriched carbonate environment promoting biological calcification
5. An active carbon sink especially in winter and spring months.

1. Introduction

Marine coastal shallow sites are extremely rich, but complex systems. They are characterised by biological richness and diversity, fluctuations in seawater physical and chemical variables (e.g. temperature, conductibility, dissolved oxygen, nutrients, light and carbonate environment) (Wolfe et al., 2020), and shallow depths (i.e., shore habitat, rocky shores, or seagrass beds (Hurd et al., 2011)).

To improve the understanding of coastal marine systems and their strength or vulnerability to climate change, Ocean Big Data gathering represents a priority. High-resolution coastal observatories with high frequency data acquisition are powerful tools for validating satellite data and models, providing real-time data necessary for making predictions on seawater changes, and thus providing early warnings for maritime activities. Nowadays, ocean observatories have expanded far beyond their traditional scientific research functions and now serve as critical connections between ocean science and society, addressing the demand to understand the connections between ocean processes, their changes and thus planning sustainable developmental strategies for its resources (Sustainable Development Goal (SDG) 14 in UNFCCC Agenda 2030 (2015); Ruhl et al., 2011), according to Blue Growth objectives.

Recognized the strategic importance of long-term ocean observation, the European Community has been funding the creation of several Research Infrastructures under the frameworks either of the European Strategy Forum on Research Infrastructures Roadmap (e.g., EMSO, EMBRC, ICOS, eLTER, see ESFRI, 2021 as a reference) or of the Horizon Infrastructural (INFRA) calls (e.g. JERICO). Besides addressing specific scientific questions, these infrastructures provide the base line to address Europe's policy demands for sustainable use of the seas, ecosystem-based management and establishment of environmental status indicators, as expressed by the EU's Marine Strategy Framework Directive (MSFD) and the Nature Restoration Law.

Among ocean data, physical-biogeochemical observations are becoming increasingly urgent given the need for quantifying the current characteristics and trends of physical and biogeochemical states, even though long term, high-resolution and comprehensive data are still very rare. Relevant at global, regional and local scales (Fennel et al., 2019), such data provide estimates of the carbon cycle, acidification, primary production, and oxygen and nutrient availability affecting local ecosystems. However, long term, high-resolution and comprehensive data are still very rare especially in some areas of the Mediterranean Sea.

Under this framework, this study presents a new high-resolution underwater coastal observatory from the Eastern Ligurian Sea (Mediterranean Sea) by analysing three years of physical-biogeochemical data driven by climate change.

The Mediterranean Sea is a semi-enclosed basin with orography, physical, biogeochemical and ecosystem characteristics extremely variable (Pinardi et al., 2015; Siokou-Frangou et al., 2010). Furthermore, the ongoing direct and indirect anthropogenic impacts are affecting such characteristics and the way they interact at different scales (Micheli et al., 2013; Giorgi, 2006). Physical data have been extensively described for the basin as well as the tendencies and projections by combining data and models (Darmaraki et al., 2019; Marullo et al., 2023), but biogeochemical data from *in situ* observations are very limited, tendencies are almost absent and generally related to single variables (as chlorophyll (Chl-a)). Satellite data for the period 1998–2009 revealed significant positive Chl-a trends in most of the western Mediterranean and negative trends in the northern Adriatic Sea (Colella et al., 2016) highlighting different regional and local dynamics. In the Mediterranean basin, the carbonate system is unique due to the intrinsic seawater characteristics: warm waters and high Total Alkalinity (TA > 2500 μmol kg^{-1}) associated with a permanent and rapid thermohaline circulation loop with a residence time of nearly 100 years (Millot et al., 2005). On average, the TA in the Mediterranean Sea is 10% higher than that of the global ocean (Palmieri et al., 2015) thus giving a key role to the Mediterranean Sea in carbon sequestration.

Located in the northwestern part of the Mediterranean, the Ligurian Sea represents a key basin with a geological history closely connected with the evolution of the Western Mediterranean Sea (Migon et al., 2020). Physical observations, as current measurements and temperature-salinity (T/S) profiles, started in 1960's- '70s in the Ligurian Sea, mainly on the western part including the Gulf of Genova, and they consisted of regular monitoring campaigns from ship stations. Recently, survey stations have been implemented with buoys and profiling floats in both shallow to deep stations, as the DYFAMED station and the BOUSSOLE or W1M3A buoys (Migon et al., 2020). Data collected during the last 40 years in the Ligurian Sea have shown an increase in both temperature and salinity (the latter starting at the end of '80s), in both shallow and deep stations (Prieur et al., 2020). The origin of this trend could be explained by the waters entering the Ligurian Sea along western Corsica, confirming historical ship observations (Goffart et al., 1995; Gostan, 1968; CNRS 1973, 1975) and recent profiling floats and gliders (Bosse et al, 2015). From the biogeochemical point of view, observations in the Ligurian Sea started in 1998 with surveys up to 2016 and were successively integrated with permanent observatories with autonomous sensors for surface and deep measurements. Despite the extended knowledge on the Western Ligurian Sea, revealing a marked seasonality of the carbonate system characterizing (Coppola et al. 2020, Migon et al. 2020), the biogeochemistry of the Eastern Ligurian Sea is still poorly known.

To fill this knowledge gap, in 2021 we established Smart Bay Santa Teresa underwater observatory, a new *in situ* coastal high-resolution system located in the eastern Ligurian Sea. Physical and biogeochemical data were collected from 2021 and 2024 with the aims to: (1) describe physical and carbonate environments, (2) detect effects of physical and biological components on the carbonate environment, and (3) identify changes in marine heatwave patterns.

High-resolution Smart Bay Santa Teresa dataset enables analysis of real-time changes at local scales, highlighting the complex dynamics and relevance of coastal sites where seawater, atmosphere, and biological systems mutually interact. Data are discussed with the perspective of the observatory empowerment (i.e., more stations and more variables measured) aiming at providing continuous, long-term datasets understanding the link between biogeochemical patterns and ecological responses and thus predicting the fate of coastal ecosystems under climate change.

2. Material and methods

2.1. The study area

The study area is located in the Gulf of La Spezia from 43.95 °N, 9.64 °E to 44.15 °N, 10.05 °E, with depth from 8 to 25 m (Fig. 1). The area is located between the Magra River mouth and the Cinque Terre National Park.

The continental shelf of the Ligurian Sea has a limited extension along all the Liguria region until the Gulf of La Spezia. Its eastern deeper part is characterised by the Levante Canyon, almost parallel to the coast and hosting valuable and vulnerable ecosystems, such as the deep-living cold-water corals found from 500 m of depth (Fanelli et al, 2017). The canyon area was studied with a deep submarine multidisciplinary observatory positioned at 608 m depth whose data showed the presence of two main water masses: the surface water of Atlantic origin (Atlantic Water, AW; upper 150 m), well separated from the underlying intermediate water, and the Levantine Intermediate Water (LIW) that occupies the layer between 200 m and 500–700 m depth (Ciuffardi et al., 2023). Historical hydrographic monitoring carried out by ENEA since the ‘80s (in situ stations and periodic campaigns) and observations on current dynamics done by Gasparini et al. (2009), allowed to characterise physical conditions of the area. The 40-year daily climatology of the nearest grid point of the area (Merchant et al., 2019; Saha et al., 2018) shows a mean surface seawater temperature of 18.5 ± 4.3 °C, ranging from 13.0 °C to 25.4 °C.

The coastal area is affected by deep circulation dynamics, characterised by an East-West cyclonic flux. In particular, the Eastern Ligurian Sea receives waters flowing towards North from both sides of Corsica Island: warm waters coming from the Tyrrhenian Sea through Corsica channel and cold waters rising from the Western Mediterranean current. These two circular fluxes merge and originate a current with intermediate properties at the North of Corsica Island. Seasonal variations characterise Eastern Ligurian circulation: a single large-scale cyclonic circulation occurring in winter is transformed into complex circulation patterns in summer. However, a vast variety of oceanographic dynamics are still unsolved in this area, as recent water property evolution across the Corsica Channel, in the Liguro-Provencal Current and the Western Corsica Current or the water mass modifications due to climate change and their relationship with the deep-water formation in the Gulf of Lion (Aracri, 2019). The circulation in the Gulf of La Spezia is the result of the combined effects of interior dynamic and large-scale flow, also considering the dam of the port of La Spezia with a length of 2.2 km, that separates the Gulf from the open sea. An inflow/outflow along the open boundary off the dam is described for the surface layer, with a prevalence of the outflow, mainly concentrated along the western opening (Gasparini et. al., 2009).

In the Gulf, dominant winds are from North and North-East, whereas Scirocco (South-East) is responsible for the strongest sea-storms (Bordone, 2019).

The area's biological and economic relevance (e.g. mollusc farming, fishing, aquaculture) makes it an ideal site for coastal monitoring and protection (Peirano et al., 2011; Cocito and Sgorbini, 2014; 2012; Ragazzola et al., 2021): marine coastal ecosystems of the Gulf of La Spezia and surrounding Marine Protected Areas (Cinque Terre National Park, Natural Regional Park of Porto Venere and Natural Regional Park of Magra-Vara – Montemarcello) are very diverse such as coralligenous habitats, Posidonia meadows, bioconstructional shallow calcifying ecosystems. Furthermore, the Gulf is characterized by a strong dual use, as natural environments coexist with highly impacted areas such as a military and a commercial harbour and marinas. The Gulf hosts Navy bases and several maritime activities of national economic relevance, as naval trade, shipbuilding, cruise terminals, also supporting the need for a long-term monitoring.

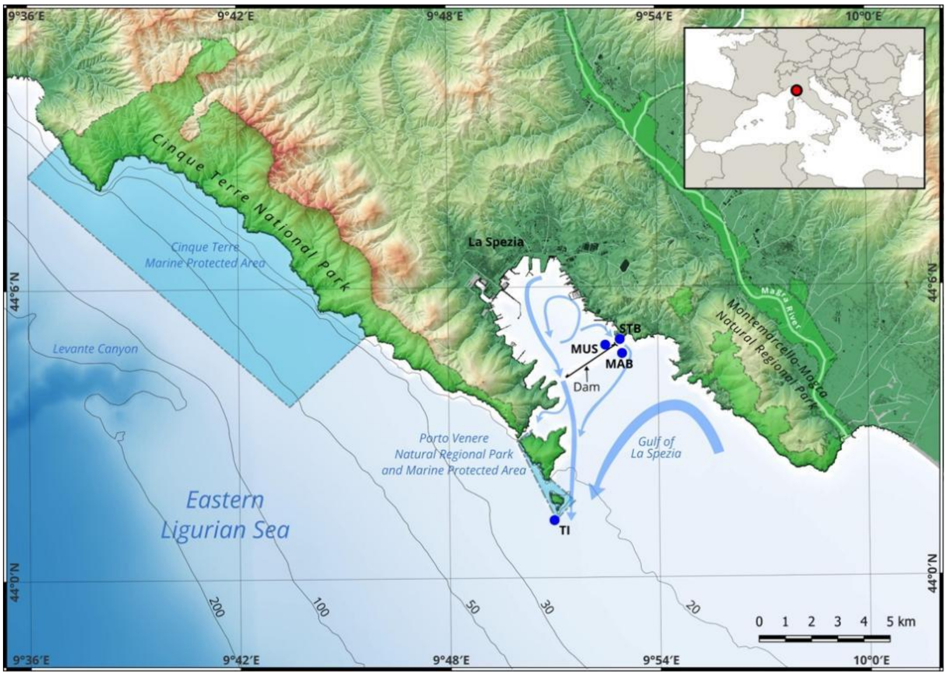

Fig. 1. The study area with Santa Teresa Bay (STB) (depth: 1 m), Mussel inner station (MUS) (depth: 5 m), Mussel Aquaculture Buoy (MAB) (depth: 5 m) and Tino Island (TI) (depth: 1, 5 and 16 m) stations shown as blue circles. Qualitative surface circulation scheme of the Gulf (arrows) as described by Gasparini et al., 2009.

2.1.1. Smart Bay S. Teresa observatory: in situ *measurements and stations*

Smart Bay Santa Teresa (SBST) is a cooperation platform established between research institutes (ENEA, CNR and INGV), local administration (Municipality of Lerici) and local stakeholders (Scuola di Mare and Cooperativa Mitilicoltori Associati) to develop a natural laboratory combining research, technology, sustainable tourism and shellfish farming. Among SBST's aims, there is the creation of an autonomous intelligent observatory as a model for big data production in coastal areas by using advanced technologies, working on data validation *via* analytical methods, and ultimately correcting the acquired data by Artificial Intelligence (AI) (Ma et al., 2022; Durin et al., 2023; Ferri et al., 2024). Based on innovative technology, SBST observatory included four stations equipped with multiparameter probes and/or sensors and gathering high-resolution data: 1. Santa Teresa Bay (STB) (depth: 1 m) leisure marina inside the dam; 2. Mussel Aquaculture station (MUS) (depth: 5 m) inside the harbour; 3. Mussel Aquaculture Buoy (MAB) (depth: 5 m) outside the harbour; 4. Tino Island (TI) (depths: 5 m and 16 m) in the Regional Park and outside the Gulf.

The SBST stations were positioned along an anthropic gradient, from the harbour to the external side of the Regional Natural Park of Porto Venere (Fig. 1). In particular:

- STB (44.0819°N, 9.8817°E). The station was located inside Santa Teresa Bay, a small bay on the east side of the harbour, inside the dam. The bay, approximately 80 m long and 80 m wide, is a natural bay hosting a sailing school and the mussel farm. Despite the vicinity of the harbour, the bay maintains its natural character, hosting calcifying marine ecosystems (mussels, algae, bryozoans, corals, gorgonians) and native plants on land. It is part of a Nature 2000 site. The underwater station (see Tab. 1) was positioned at 1 m of depth on a floating pontoon (max sea-bottom depth = 8 m) where each single measurement instrument was connected to an underwater acoustic node (WNodes, WSense s.r.l., Italy) acquiring and transmitting data every 30 minutes.

- MUS (44.0791°N, 9.8744°E). The station was positioned at the eastern corner inside of the dam in proximity to the mussel aquaculture field. This station was located at 5 m of depth and was composed of a single measurement instrument, a current meter, connected to an underwater acoustic node (WNode) acquiring and transmitting data every 30 minutes.
- MAB (44.0771°N, 9.8808°E). The station was positioned at the eastern corner outside of the dam in proximity to the mussel aquaculture field. The monitoring station was positioned on a buoy at a depth of 5 meters (in an area with a maximum seabed depth of 11 meters). It utilized two WNodes, each connected to different measuring instruments, to acquire and transmit data every 30 minutes.
- TI (44.0198°N, 9.8502°E). The station was positioned in the Regional Park of Porto Venere outside the Gulf, located on the southwest side of Tino Island. This station was located on a buoy at 16 m of depth. The instrument positioning was primarily driven by logistic constraints since the buoy had a jumper at 11 m of depth, thus making it too risky the positioning of any scientific instruments above it. This station was the least anthropogenically impacted for the area. The sea bottom (max depth: 25 m) is muddy but the islands offer rocky walls that host a remarkable biodiversity and the animal forests characterizing the coralligenous habitat with species of high ecological value for the Mediterranean Sea, such as *Paramuricea clavata*, *Eunicella* sp. *Lophogorgia sarmentosa*, *Pentapora fascialis*, *Cladocora caespitosa* (Bramanti et al., 2016; Lombardi et al., 2020) here starting at 15 m of depth due to the peculiar environmental conditions. This station provides data that support the annual ecological monitoring of the Regional Park, and its calcifying marine ecosystems are part of the Eastern Ligurian Site of the eLTER Network).

Physical high-resolution data (temperature (t), practical salinity (SP), dissolved oxygen (DO), current, fluorescence, turbidity, Chl-a) have been acquired from October 2021 to August 2023 via *in situ* sensors. Real-time data transmission was based on Internet of Underwater Things (IoUT-WSense) wireless network technology, acquiring and transmitting data every 30 minutes at STB, MUS, and MAB stations.

Biogeochemical data were measured analytically (total alkalinity (TA), total scale pH (pH_T)) and calculated (partial pressure of carbon dioxide (pCO_2), carbon dioxide (CO_2), dissolved inorganic carbon (DIC), calcite and aragonite saturation states (Ω_{Ca}, Ω_{Ar})), with a weekly sampling frequency at STB, and monthly at MAB and TI. High-precision data profiles (measured by means of a Conductance-Temperature-Depth probe, CTD) were also collected as detailed in Table 1.

Hydrodynamic conditions were recorded from 18th of October 2021 to 26th of June 2023 by single-point current meters located at 5 m of depth outside and inside the dam of La Spezia port (MAB and MUS stations in Fig. 1, Tab. 1).

In addition, a meteorological station, located at an altitude of 49.5 m in the same area and operated by ENEA, collects solar radiation, atmospheric pressure, air temperature, wind direction and speed, and relative humidity every 10 minutes (Bordone, 2019).

Table 1. Environmental parameters acquired in each station (STB, MUS, MAB and TI) at different time intervals (minute, hour, week, month) by means of *in situ* measurements - with probes and sensors - and analytical methods. ∞ Stations connected with underwater communication technology (WNodes, WSense, Italy); * pH_T: pH total scale. ** carbonate environment derived (Jiang et al., 2014); *** dissolved oxygen analytically measured via Winkler titration method (Bryan et al., 1976; Winkler,1888). Physical variables: *t*, O_2, *p* (pressure), S_P, *C* (conductivity), Chl-a (chlorophyll-a), fluorescence, turbidity, current speed and direction. Chemical variables: pH_T, TA, pCO_2, DIC, Ω_{Ca}, and Ω_{Ar}. Nutrients: NO_3 (nitrates), NO_2^- (nitrites), $Si(OH)_4^-$ (silicates), PO_4^{3-} (phosphates)

Parameters	**Instruments/ Sensor/Software**	**Measurement depth**	**Data Frequency**
Station ∞ STB Coordinates 44.081871°N 9.881686°E			
t, C	Conductivity Sensor 4319, AANDERAA, Norway		30 min
DO	Optode 4531, AANDERAA, Norway		
t, C, p, DO, S_P	SBE19plus, SeaBird Electronics Inc., USA		
pH_T, t	Seven-Go, Mettler Toledo, USA		weekly
TA	HI 901C, Hanna Instruments, Italy	1 m	
****pCO_2, CO_2, DIC, Ω_{Ca}, and Ω_{Ar}**	CO2SYS-Excel		
NO_3^-, NO_2^-, $Si(OH)_4^-$, PO_4^{3-}	Braan+Luebbe, Germany		
*****DO***	794 Basic Titrino Metrohm, Italy		
Station ∞MUS Coordinates 44.079140°N 9.874360°E			
current speed and direction	Z-Pulse 4420, AANDERAA; Norway	5 m	30 min
Station ∞MAB Coordinates 44.077130°N 9.880829°E			
DO	Optode 4531, AANDERAA, Norway		30 min
current speed and direction	Z-Pulse 4420, AANDERAA; Norway		
t, C, p, DO, S_P	SBE19plus, SeaBird Electronics Inc., USA		
pH_T, t	Seven-Go, Mettler Toledo, USA	5 m	
TA	HI 901C, Hanna Instruments, Italy		monthly
****pCO_2, CO_2, DIC, Ω_{Ca}, and Ω_{Ar}**	CO2SYS-Excel		
NO_3^-, NO_2^-, $Si(OH)_4^-$, PO_4^{3-}	Braan+Luebbe, Germany		
*****DO***	794 Basic Titrino Metrohm, Italy		
Station TI Coordinates 44.019788°N 9.850245°E			
t	OnSet HOBO WaterTemp Pro V2	5 m	

t, C, S_P, p, O_2* and *pH_T	SeapHOx, SeaBird Electronics Inc., USA	16 m	60 min
t, C, p, DO, S_P	SBE19plus, SeaBird Electronics Inc., USA	1 m, 16 m	monthly
****pH_T, t***	Seven-Go, Mettler Toledo, USA		
TA	HI 901C, Hanna Instruments, Italy		
*****pCO_2, CO_2, DIC, Ω_{Ca}, and Ω_{Ar}***	CO2SYS-Excel		
NO_3^-, NO_2^-, $Si(OH)_4^-$, PO_4^{3-}	Braan+Luebbe, Germany		
******DO***	794 Basic Titrino Metrohm, Italy		

2.1.2. Underwater communication via *Internet of Underwater Things*

The stations STB, MUS and MAB were connected to the underwater communication network via an innovative adaptive underwater wireless network provided by Wsense. In particular, the WSense system in Smart Bay S. Teresa Observatory consisted of underwater nodes (WNodes) able to create a wireless mesh network communicating acoustically to collect data from sensors and then route them up to a WGateway, a device acting as a bridge between the underwater and terrestrial domain. The collected data are then forwarded to the Internet through a 3G/4G mobile connection and stored in the WCloud, a dedicated web-space created by WSense for the observatory system that allows real time visualisation for the users (i.e., researchers). Through the WGateway it is possible not only to receive data but also to send commands to the WNodes to change sampling frequency, configurations, etc. in real-time. The WGateway, located in the mussel farm building, was equipped with an underwater cable (30 m) ending with an acoustic modem deployed at 3 m of depth on the sea bottom to operate the underwater network. To guarantee the data communication with the most distant nodes (i.e., MAB and MUS stations), two nodes were positioned at 5 m of depth under the floating barriers in Santa Teresa Bay (Fig. 1) acting as network relays. Communication is bidirectional (to/from sensors) which allows to reconfigure the application logic of the sensor nodes upon need. The adaptive protocols, designed and implemented dynamically, change the route for data delivery as well as the data link layer parameters in presence of harsh channel conditions, in this way being able to reliably deliver both data and control information in noisy shallow water underwater communication environment.

2.2. Biogeochemical and physical analytical measurements

2.2.1. Carbonate environment

The marine CO_2 system involves a series of interconnected equilibria constituting the dominant buffering system in the ocean that somewhat resists anthropogenically induced acidification due to the increased concentration of atmospheric CO_2. Figure 1S, in Supplementary Material, reports a simplified scheme of reactions and processes determining the concentration of the species related to the carbon cycle in sea water. The inorganic carbon system can be described by four interlinked parameters: TA, DIC, pH, and pCO_2. By directly measuring two of these four parameters, utilizing equilibrium constants specific to the nature of the aquatic system of study, as well as supplying data on temperature, salinity, pressure and specific inorganic seawater constituents, it is possible to calculate the remaining two parameters and also the saturation states (Ω), for both aragonite (Ω_{ar}) and calcite (Ω_{cal}) (Zeebe, 2012).

For total alkalinity (TA) measurements, three replicated samples were collected using the Go-Flo bottle and stored into acid-washed 0.250 L borosilicate glass bottles. Samples were poisoned with 50 μL of a 70 g/L $HgCl_2$ and analysed within a week. Measurements of TA were performed by potentiometric acid titration with open cell following the methods described by Dickson et al., 2007 by using an automatic titrator equipped with a pH glass electrode/reference electrode cell (Tab. 1). An accurately measured 160 g of seawater was titrated at constant temperature of 25.0 ± 0.5 °C in open cell with a standardised solution of hydrochloric acid (HCl 0.1 N) with salinity adjusted to 38 with NaCl in order to be similar to the samples one. The sample was acidified to a pH of about 3.5 with a single accurately measured aliquot of titrant, then stirred for 10 min to allow for the liberation of the CO_2 that had evolved. The titration continued by adding 0.1 mL of titrant and reading the mV until a pH of about 3.0 was reached. TA was computed from the titrant volume and potential difference measurements using a non-linear least-squares approach (Gran method) proposed by Dickson et al., 2007. The reproducibility of the three measurements on the same sample was ± 2 μmol/kg Routine analyses of Certified Reference Materials (batch # 165, provided by A. G. Dickson, Scripps Institution of Oceanography) ensured the accuracy of the measurements (better than ± 4 μmol/kg).

The pH_T was determined by electrometric measurements with standard T31 Dickson TRIS Buffer Solution in Synthetic Seawater (Dickson et al., 2007; Paulsen and Dickson, 2020) by using Mettler Toledo pH meter equipped whit glass electrode. The Nernstian answer of glass electrode was verified before the measurements on samples by buffered solution. The pH_T at sea water temperature was calculated by DelValls and Dickson (1988) equation. The estimated uncertainty in pH_T measurements is ±0.01 pH. By considering the maximum uncertainty in pH and TA the overall uncertainty in the derived pCO_2 is ± 15 μatm.

Seawater carbonate system parameters were derived from TA and pH values. Calculations were made with the software program CO2SYS-Excel (https://github.com/jamesorr/CO2SYS-Excel/blob/master/CO2Sys.xls). Specifically, as recommended for the Mediterranean Sea by Álvarez et al. (2014), the carbonic acid dissociation constants K_1 and K_2 from Mehrbach et al., 1973 as refitted by Dickson and Millero, 1987 and the dissociation constant for HSO_4^- from Dickson, 1990 were used. Uppström, 1974 was used to calculate the ratio of total boron to salinity and Dickson and Riley, 1979 to calculate the hydrogen fluoride constant K_F.

To distinguish the effects of temperature and biological processes on pCO_2 in surface seawater, thermic (T) and non-thermic (i.e., biogenic, B) pCO_2 have been calculated by following the approach described by Takahashi et al., 2002.

Thermic pCO_2 and non-thermic pCO_2 are calculated by the following equations:

$$\textit{Thermic } pCO_2 = T = pCO_{2mean} \exp\left[0.0423(T_{obs} - T_{mean})\right]$$
$$\textit{Non-Thermic } pCO_2 = B = pCO_{2obs} \exp\left[0.0423(T_{mean} - T_{obs})\right]$$

Where pCO_2 mean is the mean pCO_2 retrieved by CO2SYS over the study period, $pCO_{2\ obs}$ is the retrieved pCO_2 at each point of pH_T and TA measurements, T_{obs} is the measured temperature, T_{mean} is the mean temperature measured in the periods. The value of 0.0423 was empirically derived by Takahashi et al., (2002).

The effect of temperature changes on the mean annual pCO_2 value:

$$(\Delta pCO_2)_{temp} = (\textit{Thermic } pCO_2)_{max} - (\textit{Thermic } pCO_2)_{min}$$

The effect of biology on the surface-water pCO_2 is:

$$(\Delta pCO_2)_{bio} = (\textit{Non-Thermic } pCO_2)_{max} - (\textit{Non-Thermic } pCO_2)_{min}$$

The ratio $T/B = \Delta pCO_{2temp}/\Delta pCO_{2bio}$ is then calculated to study the dominant process affecting pCO_2 in superficial sea water.

2.2.2. Inorganic nutrients

Samples for inorganic nutrients (NO_3^-, NO_2^-, $Si(OH)_4^-$, PO_4^{3-}) were collected at 1 m of depth with a 2L Go-Flo bottle and stored in 20 mL polyethylene bottles. Since it was not possible to carry out the analyses immediately, samples were frozen just after the sampling and kept frozen (-20 °C) until the analysis. All nutrient samples were analysed by using a standard colorimetric method on a segmented flow analyser (Tab. 1), according to the classical methods described in Grasshoff and coauthors (1983). Measurements were performed at maximum 1 year after the sampling. The reproducibility of the measurements of standard solutions was always from 5% to 10%.

2.2.3. Winkler method

Discrete samples were periodically collected to calibrate the high precision dissolved oxygen (DO) data profiles recorded by the CTD sensor. The in-situ samples are needed to fulfil quality assurance standards and correct any potential bias and drift in the SBE 43 oxygen sensor, following Janzen et al. (2007) and Uchida et al. (2010). The calibration procedure is based on the Winkler titration method (Grasshoff et al. (1983), Langdon, 2010). It is based on the reaction of O_2 with manganese (II) ions in alkaline solution and subsequent oxidation of iodide to iodine after acidification. Iodine is back titrated with standardized thiosulphate in acid solution. The endpoint is then detected at the ENEA Laboratory using automated methods by means of a Metrohm Titrino 794.

2.3. Satellite Sea Surface Temperature (SST) and Marine Heatwaves (MHW)

SST data were downloaded from the Copernicus Marine Environment Monitoring Service catalogue (CMEMS, COPERNICUS). The database corresponds to SST_MED_SST_L4_REP_OBSERVATIONS_010_021 (Merchant et al., 2019; Saha et al., 2018), which has a resolution of 0.05 °C and covers the period from 25 August 1981 to 21 October 2024. We selected the period 1982 - 2023, as data discussed in the present paper extend to August 2023. These data were obtained by combining Pathfinder V5.3 (PFV53) AVHRR data with a bias-corrected version of the CMEMS NRT L4 data up to 2017 to provide a full time series of consistent daily gap-free maps (L4) at the original PFV53 resolution (0.0417° x 0.0417°). The data provide a stable and consistent long-term SST time series over the Mediterranean Sea developed for climate applications and were interpolated through an Optimal Interpolation algorithm on the original Pathfinder grid (at 0.0417° x 0.0417° spatial resolution). They were representative of night SST values (00:00 UTC) (coordinates of the points: 44.0688°N 9.9007°E/ 44.0688°N 9.8507°E / 44.0187°N, 9.8507°E selected as the nearest grid point to STB, MAB and TI respectively). Results were shown to be comparable and hence main analyses are only shown for TI station, as being in correspondence with the carbonate reef site and closest to the respective CMEMS grid point (i.e., more comparable to its climatology).

Following Hobday et al. (2016), the 90th percentile of the SST anomaly was calculated to define the MHW threshold, referring to the 40-year daily climatology. A MHW has been assumed when the anomaly showed values above the threshold for at least five consecutive days. A frequency function was computed for defining the representative area:

$$f_{site}(x,y) = \frac{\sum_{t=1}^{T} \frac{|c(x_{site}, y_{site}, t) - c(x,y,t)|}{SST(x_{site}, y_{site}, t)}}{T}$$

where x and y are the coordinates of the point, x_{site} and y_{site} are the coordinates of the TI station, t is the time, SST is the surface seawater temperature and T is the sum of all times. The equation compares the temperature of the TI station with the temperatures of the closest grid point of the SST_MED_SST_L4_REP_OBSERVATIONS_010_021 dataset. Anomalies computations have been performed dividing the time-series by seasons (considering quarterly slots for each season i.e., January, February and March for winter). SST climatology as well as the occurrences of MHW for winter and summer were computed on SST data. Then, starting from the anomaly’s computations on the 40-year daily climatology, MHW have been computed for the measuring stations.

3. Results

3.1 Temperature records and Marine Heatwaves

The 40-year satellite SST record close to the carbonate reef site revealed an increase in temperature of 0.045 ± 0.003 °C y^{-1} (Fig. 2).

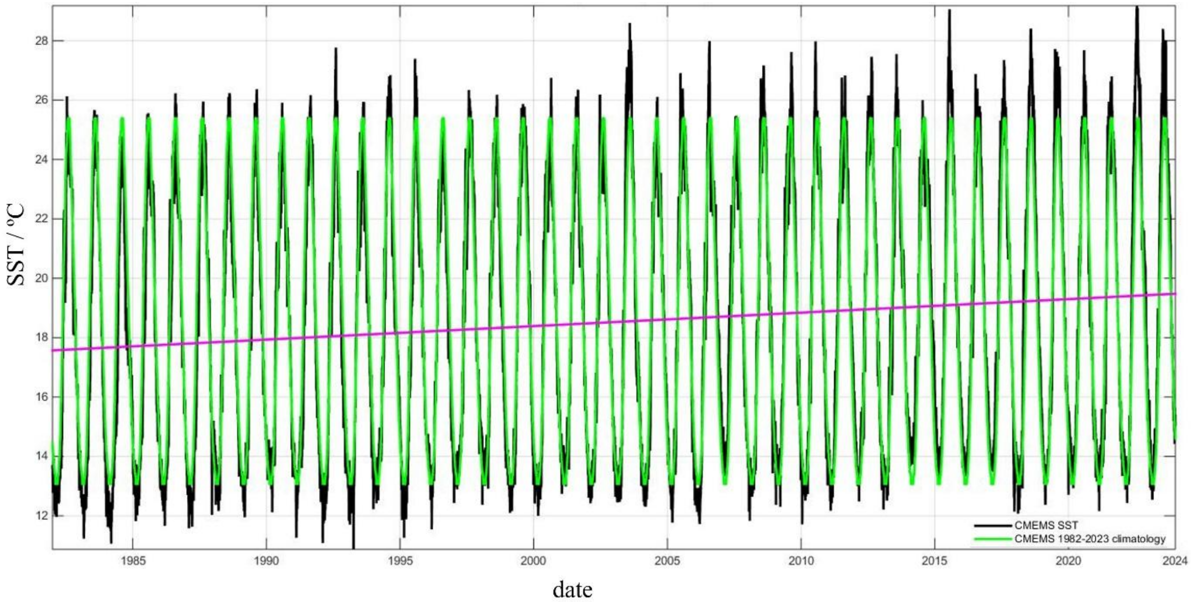

Fig. 2. The 40-year satellite SST record in black vs the climatological year in green: the increase in temperature is 0.045 °C y^{-1} as shown by the pink line. SST have been extracted from CMEMS at coordinates 44.0187°N, 9.8507°E (i.e. the nearest grid point to station TI).

Air and seawater temperatures displayed similar seasonal variations over the course of the year.
In general, there is a good agreement between long-term seawater temperature measurements at three stations and satellite SST data from CMEMS (Fig. 3). SST records were higher than SBST records only in July-August 2022. Mean daily air temperature (± standard deviation [S.D.]) in 2021-2023 was 16.2 ± 6.4 °C, ranging from 3.1 °C at the beginning of February 2023, up to 29.3 °C at the end of July 2023. For the same period, mean (± S.D.), maximum, and minimum values for seawater temperatures collected at the carbonate reef site (i.e., TI station) were 19.0 ± 5.0 °C, 28.4 °C and 11.5 °C, respectively. Maximum seawater temperature was recorded at the end of July 2023 (2 days later the warmest recorded air temperature), while the minimum was recorded on mid-February 2023 (9 days later than the coldest recorded air temperature).

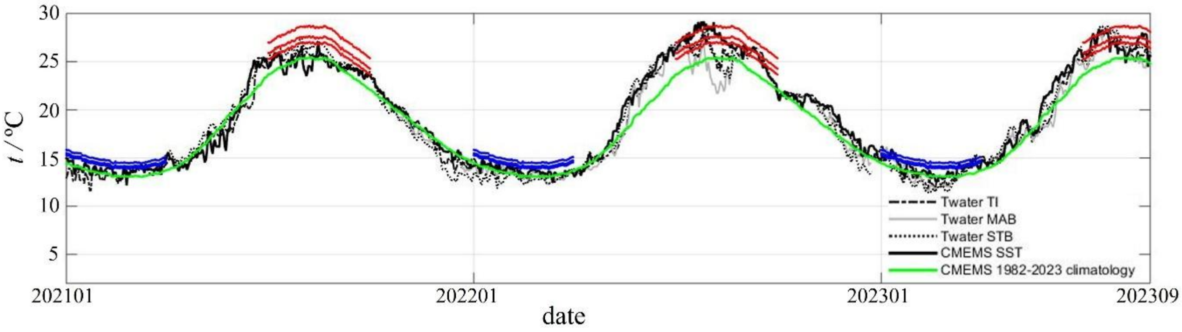

Fig. 3. Temperature time series. Trends of CMEMS SST (black solid line) and seawater temperatures (dashed and grey lines) measured at the STB, MAB and TI sites from 01 January 2021 to 31 August 2023. Red and blue lines show the 90th/95th/99th percentiles of the summer and winter SST anomalies respectively, referring to the 40-year daily climatology. The 90th percentile of the SST anomalies has been calculated to define the MHW threshold in the present paper, according to Hobday et al. (2016).

Focusing on the TI station (Fig. 4), a total of 7 MHWs (Hobday et al., 2016) occurred between 2021-2023 predominantly distributed in summer and with no events in 2021. The length of the summer MHWs spanned from 5 to 20 days, while the longest in winter was less than 15 days. Anomalous temperatures occurred when the values were above the daily climatology by 1.6 °C and 0.9 °C in summer and winter, respectively. Climatological values for the summer temperatures ranged between 21.8 °C and 25.2 °C, with a mean of 24.1 °C. For winter temperatures, the range was between 12.2 °C and 13.9 °C, with a mean of 12.9 °C. Between June 2021 and September 2023, a total of five MHWs occurred (green circles, Fig. 4). Regarding winter 2023, two MHWs occurred from the 1st to the 17th of January and from the 23rd to the 27th of March. Whereas in summer 2022, four MHWs occurred, from the 1st to the 15th of July, from the 23rd to the 27th of July, from the 30th of August to the 4th of September and from the 6th to the 19th of September 2022, respectively. For the monitoring period, the longest MHW (21days) occurred in July 2023, with a maximum temperature anomaly of +3.6 ◦C in relation to daily climatology, and the shortest (5 days) occurred in March 2023 with a maximum temperature anomaly of +1.7 ◦C with respect to daily climatology.

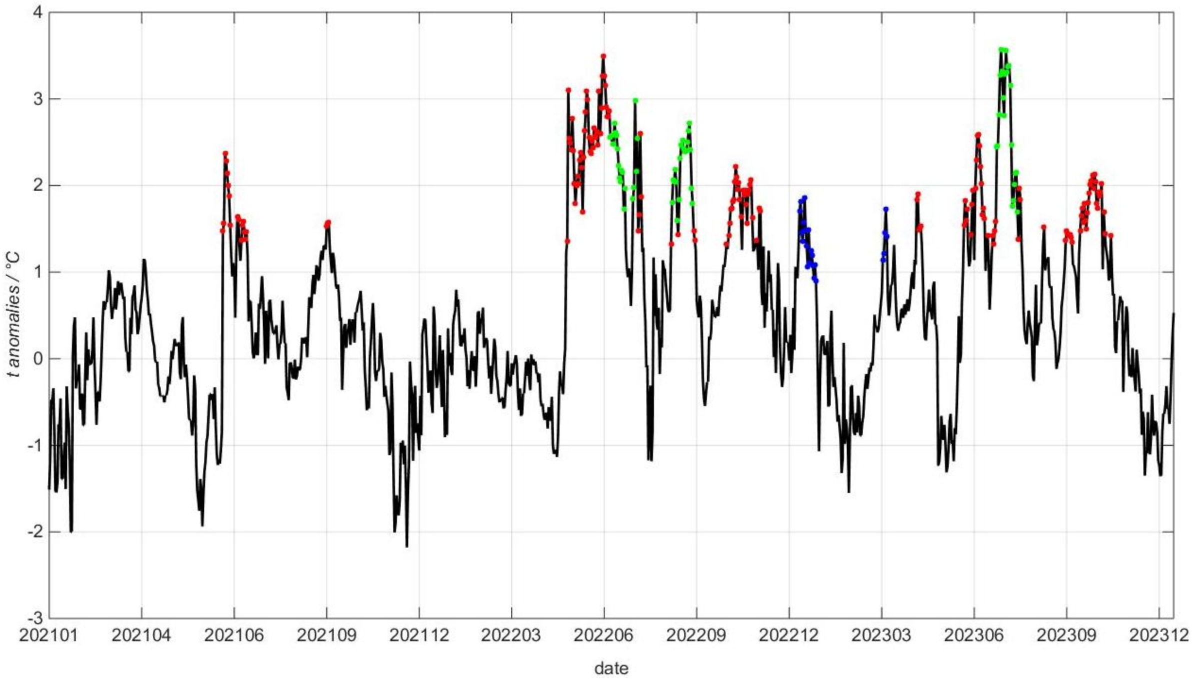

Fig. 4. MHW from 01 January 2021 to 31 August 2023. Red points show the single-day anomalies above the threshold. Green points indicate summer MHWs, when the value was above 1.6 °C with respect to the daily climatology for five consecutive days. Blue points indicate winter MHWs, when temperatures were above 0.9 °C with respect to the daily climatology for five consecutive days (Hobday et al., 2016).

3.2 Hydrodynamic records and current

Hydrodynamic data are recorded inside and outside the dam of la Spezia (Fig. 1, Tab. 2).

Table 2. data acquisition (DAQ) efficiency of both the current meters, their mean depths in the considered period (with their associated standard deviation) and the bottom depths (in brackets); the transmission efficiency of the single node (whose nominal sampling rate is equal to 1 datum every 30 minutes) takes into account both the unavoidable acoustic transmission problems (which occasionally lead to around 5% loss of the communicated data) and the suspension periods due to maintenance of the nodes themselves (e.g. battery change, firmware updates, etc.).

Station	Measured quantities	DAQ period	Mean depth [m]	Data #	DAQ efficiency
MAB	Depth &current (module and direction)	18/10/2021 to 26/06/2023	4.7 ± 0.6 (11)	15689	53 %
MUS			5.2 ± 0.4 (10)	18448	62 %

The modules and directions of currents were measured outside and inside the dam during the entire acquisition period (Fig. 5); all current data have been corrected for the effect of magnetic declination. Measures were mainly contained within a value less equal than 0.1 m s^{-1} (in 96.0% and 99.7% of cases for current measures outside and inside the dam, respectively)

Regarding current directions, measures outside the dam appeared homogeneously distributed across the four quadrants, indicating a lack of evident preferential mean direction within this module during the considered period. Stronger current values were recorded outside the dam, showing a less homogeneous distribution and a dense concentration of measurements within the 3rd-4th quadrants, with peak values (> 0.20 m s^{-1}) aligned within the 240°-345° N sector. As far as the currents inside the dam, their alignment showed a preferential direction along the W-E direction, reasonably due to the presence of the dam; higher values appeared to be contained in the sector 60°-180° N, but with values rarely greater than 0.20 m s^{-1}. The sensitivity of the measurement system was highlighted by the current data acquired during an extreme meteorological event that occurred in the Gulf of La Spezia on August 18th 2022 and shown by green circles (Fig. 5).

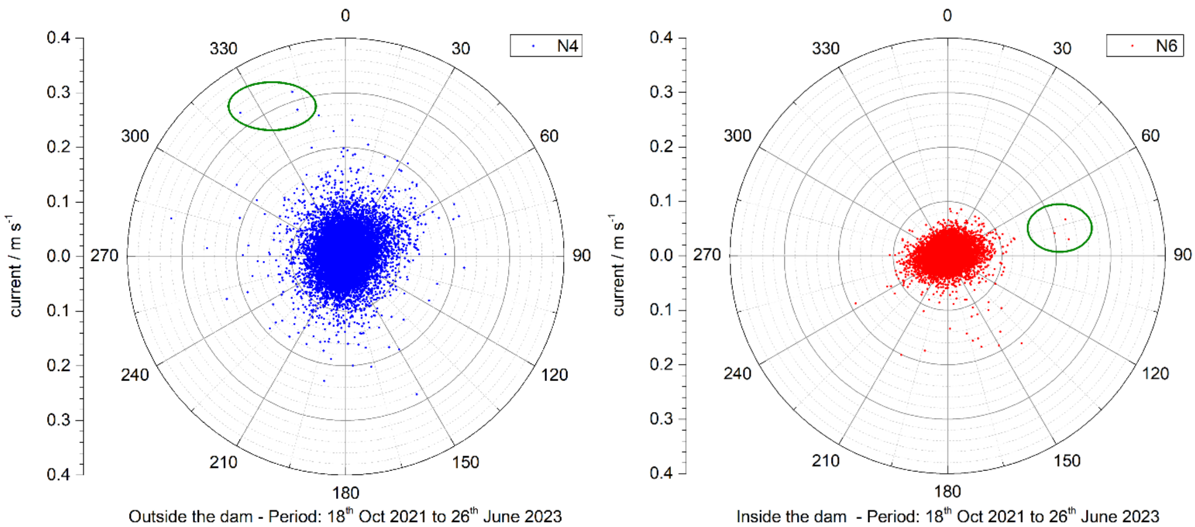

Fig. 5. Polar plots of currents measured outside (MAB, left) and inside (MUS, right) the dam. Green circles highlight data recorded during an 'extreme' meteorological event occurred in the Gulf of La Spezia.

Current intensity gets halved from outside to inside as an evident effect attributable to the dam (Fig. 6 panel a). These results are highlighted in the relative frequency histograms associated to the modules of the currents and in the distributions of the modules for both nodes (Fig. 6 panel b), showing the damping effect of the dam on water circulation.

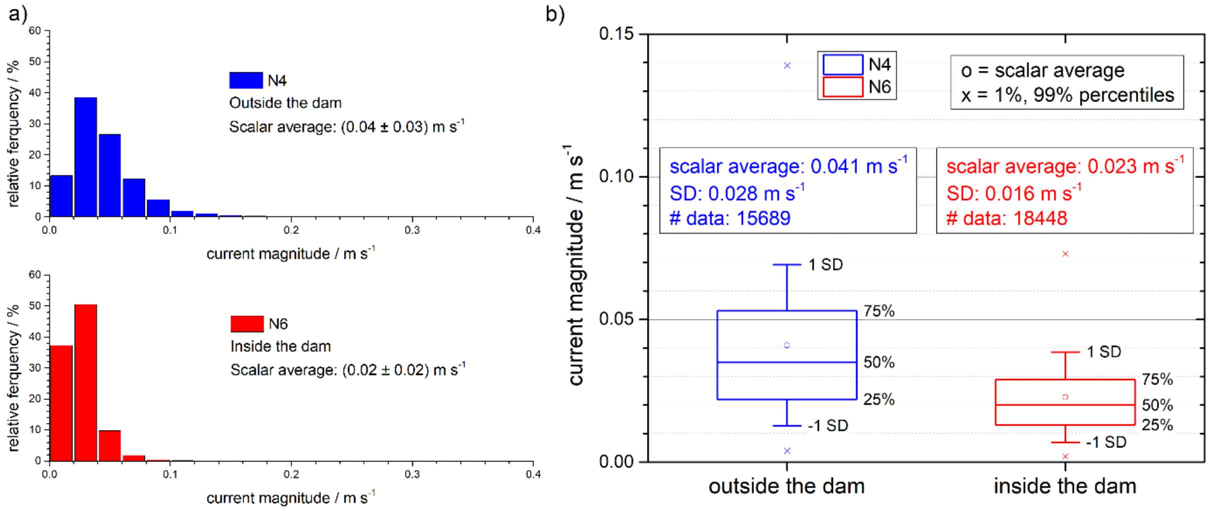

Fig. 6. Distribution of the current magnitude outside (N4-MAB) and inside (N6-MUS) the dam (a). Box plot of the current magnitude outside (N4-MAB) and inside (N6-MUS) the dam (b).

To highlight any preferential directions of the currents, the data acquired in the seawater were related to the wind measurements recorded by the meteorological station through wind-rose diagrams (Fig. 7).

Regarding the current measurements outside the dam (MAB), almost 40% of the values were distributed along the N-NE-E directions (1st quadrant), whereas the remaining values were homogeneously distributed along other directions (with a prevalence within the 3rd quadrant). This can be explained by the distribution of the winds which, in approximately 50% of the measurements, blew from S-SW. The relationship between the distribution of currents outside the dam and the winds (measured at the weather station) from a qualitative point of view, seems to be significant. The current measurements inside the dam (MUS), were distributed along the NE-E and SW-W axes in above 50% of the cases, thus confirming the influence of the dam in directing the sea current.

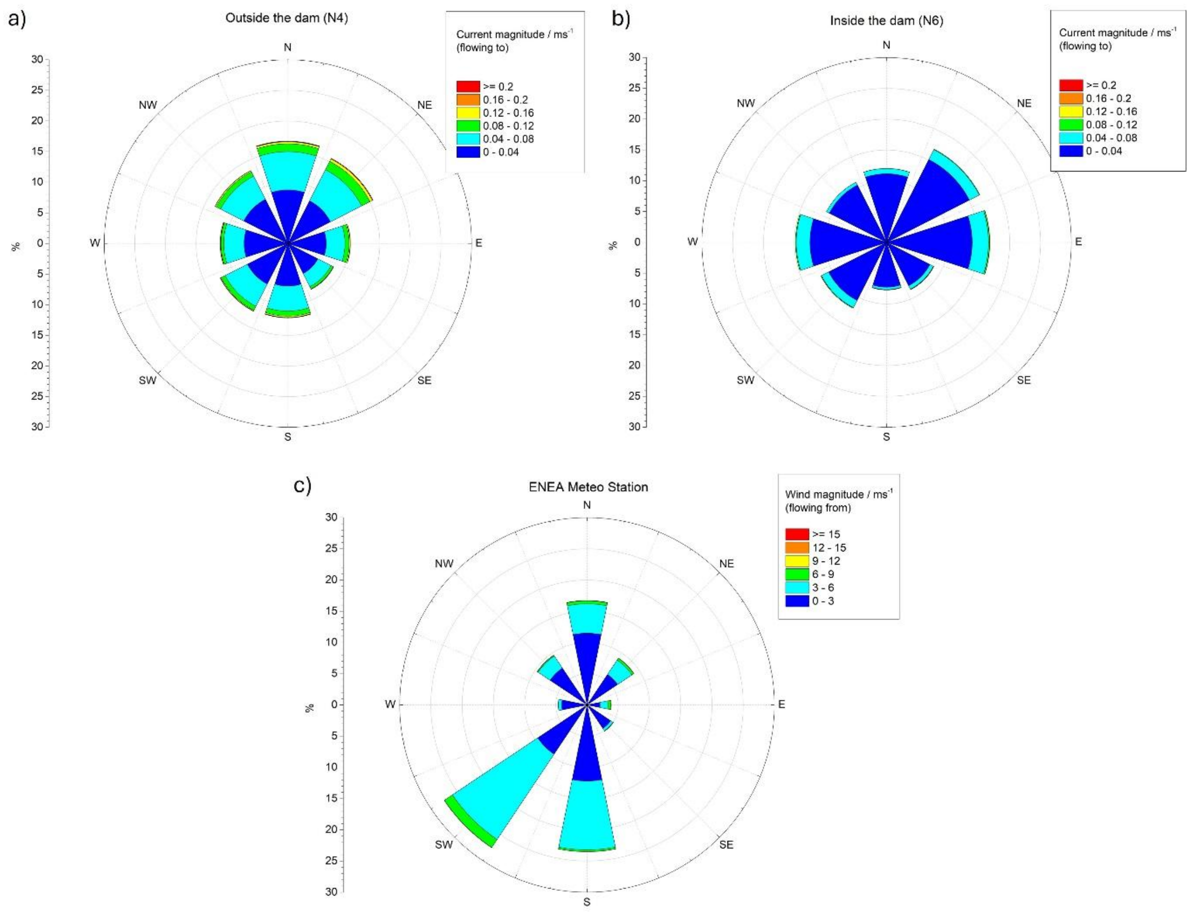

Fig. 7. (a) Distributions of current magnitude and direction outside the dam, (b) inside the dam, and (c) wind at the meteorological station. Directions follow standard conventions for ocean currents and wind.

3.4 Carbonate environment

The analysis of the whole seawater carbonate system (measured and derived) within the stations (Tab. 3) confirmed the mean TA (range: 2559- 2585 µmol/kg) of the Tyrrhenian Sea. The highest values were recorded at MAB station (depth: 5 m). DIC values ranged from 2238 to 2269 µmol/kg, with the lowest mean value at station TI (depth: 1 m) whereas pH ranged from 8.078 and 8.176 units, with the lowest value at station TI (depth: 16 m) and, interestingly, same values at stations STB and MAB (depth: 1m) and MAB (5m) with TI (depth: 1 m). Interestingly, MAB stations showed the highest pCO_2 and CO_2 values at 1 m and the lowest values at 5 m of depth. Saturation states of calcite and aragonite (Ω_{Ca} and Ω_{Ar}) showed the highest values at MAB (depth: 5m) and TI (depth: 1 m) stations, with 5.5 for Ω_{Ca} and 3.6 for Ω_{Ar} respectively, whereas the mean lowest values were recorded at MAB (depth: 1m) and TI (depth: 16 m) with 5.0 for Ω_{Ca} and 3.3 for Ω_{Ar}, the latter showing the same low values also at station STB.

Table 3. Mean and standard deviation (± S.D.) of measured and derived (*) parameters of the carbonate system (TA, DIC, pH_T, pCO_2, CO_2, Ω_{Ca}, Ω_{Ar}) at the investigated stations (STB, MAB, TI).

Mean and standard deviation (± S.D.) of measured salinity, temperature and seawater (SW) density. For each station are reported: depth of sampling and number of data (N).

	STB Depth: 1 m N= 170	**MAB** Depth: 1 m N= 9	**MAB** Depth: 5 m N= 17	**TI** Depth: 1 m N= 30	**TI 1** Depth: 16 m N= 20
Salinity	38.8 ± 1.7	37.6 ± 0.4	37.8 ± 0.4	37.4 ± 1.3	38.1 ± 0.1
Temperature (°C)	18.9 ± 5.1	18.5 ± 5.1	19.0 ± 4.0	20.2 ± 5.3	18.2 ± 3.0
SW Density (kg/m^3)	1026.3 ± 1.3	1027.0 ± 1.3	1027.1 ± 0.9	1026.4± 1.2	1027.7± 0.8
TA (μmol/kg)	2559 ± 44	2565 ± 35	2585± 24	2568 ± 42	2564 ± 31
DIC (μmol/kg) *	2265 ± 59	2269 ± 79	2261 ± 47	2238 ± 86	2261 ± 57
pH_T	8.176 ± 0.088	8.176 ± 0.112	8.104 ± 0.059	8.104 ± 0.081	8.078 ± 0.068
pCO_2 (μatm) *	425.7 ±112	443.9 ±163	380.3 ±63	384.3 ±99	407.8 ±86
Ω_{Ca} *	5.1 ±0.7	5.0 ±0.8	5.5 ±0.6	5.5 ±0.8	5.0 ±0.7
Ω_{Ar} *	3.3 ±0.5	3.3 ±0.5	3.6 ±0.4	3.6 ± 0.6	3.3 ±0.5

	STB Depth: 1 m N= 170	MAB Depth: 1 m N= 9	MAB Depth: 5 m N= 17	TI Depth: 1 m N= 30	TI 1 Depth: 16 m N= 20
Salinity	38.8 ± 1.7	37.6 ± 0.4	37.8 ± 0.4	37.4 ± 1.3	38.1 ± 0.1
Temperature (°C)	18.9 ± 5.1	18.5 ± 5.1	19.0 ± 4.0	20.2 ± 5.3	18.2 ± 3.0
SW Density (kg/m^3)	1026.3 ± 1.3	1027.0 ± 1.3	1027.1 ± 0.9	1026.4± 1.2	1027.7± 0.8
TA (μmol/kg)	2559 ± 44	2565 ± 35	2585± 24	2568 ± 42	2564 ± 31
DIC (μmol/kg) *	2265 ± 59	2269 ± 79	2261 ± 47	2238 ± 86	2261 ± 57
pH_T	8.176 ± 0.088	8.176 ± 0.112	8.104 ± 0.059	8.104 ± 0.081	8.078 ± 0.068
pCO_2 (μatm) *	425.7 ±112	443.9 ±163	380.3 ±63	384.3 ±99	407.8 ±86
Ω_{Ca} *	5.1 ±0.7	5.0 ±0.8	5.5 ±0.6	5.5 ±0.8	5.0 ±0.7
Ω_{Ar} *	3.3 ±0.5	3.3 ±0.5	3.6 ±0.4	3.6 ± 0.6	3.3 ±0.5

To understand the relationship between TA and pCO_2 and O_2 and salinity, temporal pattern occurring within the three sites were plotted (Fig. 9). The lowest salinity values (37.4-37.8) occurred at the upper seawater layers (Tab. 3), specifically at MAB (depths: 1-5 m) and TI (depth: 1m), whereas the highest values were recorded at STB and TI (depth: 16 m), with 38.8 and 38.1 respectively. The bigger data set available at STB (N= 170) allowed us to detect weekly changes in the carbonate system and in the physical environment (Fig. 8), and thus highlighting events causing a drop in salinity (approximately 1 per year, 4 in 2024, Fig. 8) and oxygen seasonal trends.

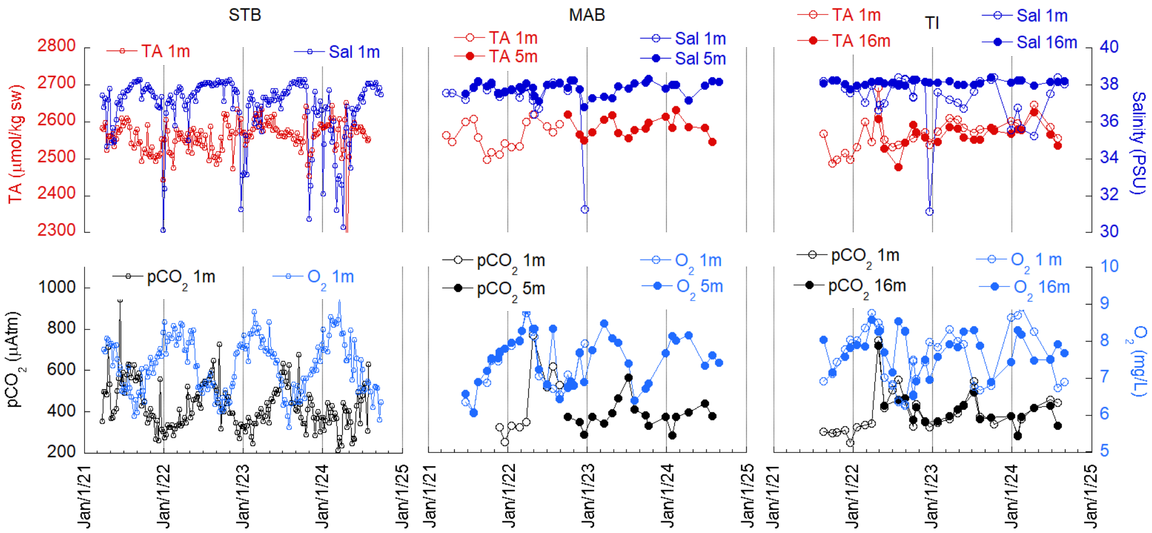

Fig. 8. Temporal patterns of total alkalinity (TA), carbon dioxide (pCO_2), salinity and oxygen (O_2) concentration in seawater at STB, MAB and TI sites. Empty dots: values acquired at 1 m of depth; full dots: values acquired at 5 m and 16 m of depth for MAB and TI, respectively. Period: February 2021- November 2024. Number of data per site: STB 1m= 170, MAB 1m = 9 MAB 5m=17, TI 1m= 30 TI 16m=20.

Oxygen concentration showed the highest peaks between February-mid March with a reduction in pCO_2 concentration, evident in STB but also in MAB and TI sites, also associated to an increase in nutrients availability (Fig. 9). This nutrient availability progressively decreased with the temperature increase; this was especially evident in late spring-summer months (Fig. 9), accompanied by a decrease in O_2 and an increase in pCO_2, revealing the effects of biological processes on the whole system.

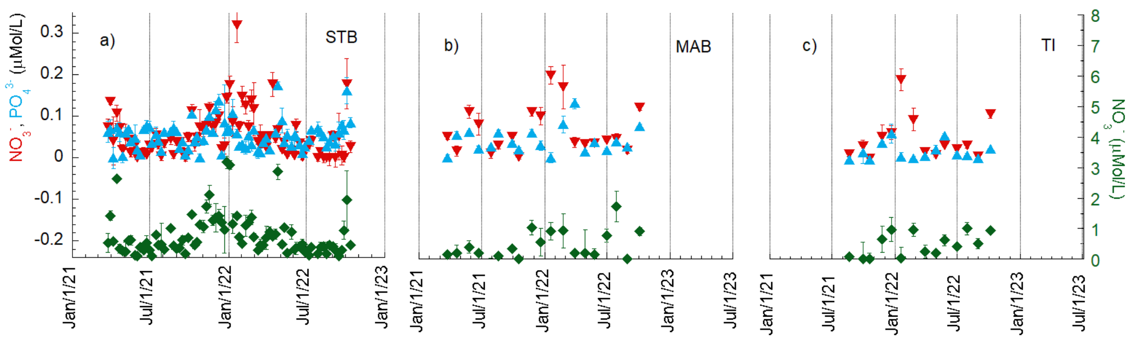

Fig. 9. Temporal patterns of nitrates (NO_3^-), phosphates (PO_4^{3-}) and nitrites (NO_2^-) concentration in seawater sample depth at STB (a), MAB (b) and TI (c). Depth: 1 m. Period: March 2021- June2023.

Figure 8 showed a great variation due to freshwater input, mixing and evaporation/precipitation influence, therefore TA and DIC were normalized (nTA and nDIC) to the mean salinity at each site using a traditional normalization style. We are aware that the tradition approach (Millero et al., 1998) could create artificial variance in distributions (Friis et al., 2003), but we chose the classical normalization since we do not have a stable endmember. Analysis of the nDIC vs nTA plot can provide useful insights into the dominant biogeochemical processes that drive the carbonate system seasonal variation (Borges et al., 2003; Krumins et al., 2013; Sippo et al., 2016; Saderne et al., 2019). The slope of the regression between nTA and nDIC follows a stoichiometric relationship that is informative of a specific metabolic pathway (Fig. 10).

Assuming that organic matter has the Redfield Ratio C: N: P, the slopes for the main biogeochemical processes that occur in the water column are: aerobic respiration = -0.2, primary production = +0.2, calcium carbonate dissolution = +2.0, calcium carbonate precipitation = - 2.0 (Krumins et al., 2013) as show by the black arrows in Figure 10. In all the three sites a significant correlation ($p < 0.01$) between nTA an nDIC and the slopes ranged from 0.427 to 0.916, indicating a combination of biogeochemical processes that affect the carbonate system of the study area. The influence of biological activity on the removal of CO_2 from superficial sea water system was very clear at STB (slope=0.916), in the other two sites the reduction of the slopes reveals the higher contribution of respiration processes especially at MAB where the lowest slope (0.427) is found.

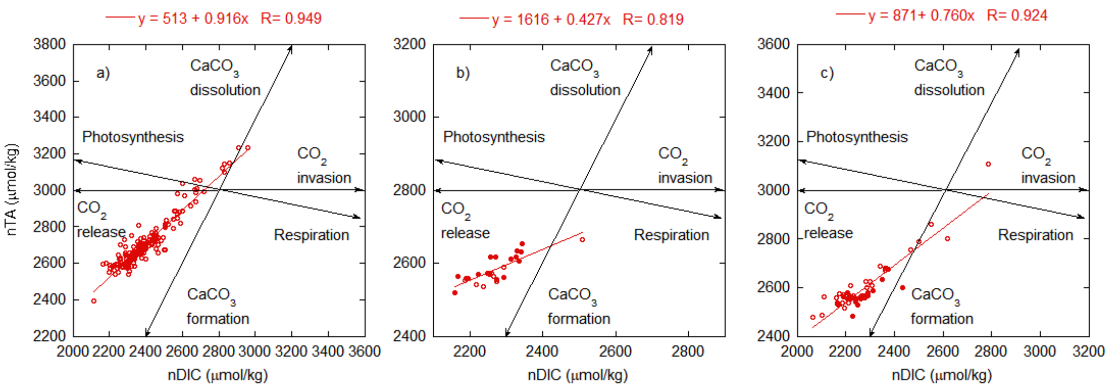

Fig. 10. Salinity normalized Total alkalinity (nTA) and Dissolved Inorganic Carbon (nDIC) plots for the three sites STB (a), MAB (b) and TI (c). Empty dots: values acquired at 1 m of depth; full dots: values acquired at 5 m and 16 m of depth for MAB and TI, respectively. For each site, regression line equation and correlation coefficient (R) are reported in red on the top of the figures. The black vectors are represented following the stoichiometric ratios of the main biogeochemical processes in order to visualize the dominant processes driving the CO_2 system.

3.3.1 Annual variability at Santa Teresa Bay

Regarding STB site, the bigger data set available (N=170) allowed the investigation of the annual variability within the carbonate system. Specifically, four TA *vs* DIC plots (Fig. 11) were drafted for those periods where pCO_2 and O_2 patterns occurred (Fig. 8).

From November to January (period=NDJ) and February to April (FMA) the highest slope were found (0.966 and 1.00 respectively) in this time period biogenic processes leading to the CO_2 removal are dominant, in the following periods (May-June-July (MJJ) and especially August-September-October (ASO) the slope become lower (0.758 and 0.429 respectively) highlighting the increased contribution of respiration processes leading to the increasing of pCO2 in sea water as observed in Figure 8.

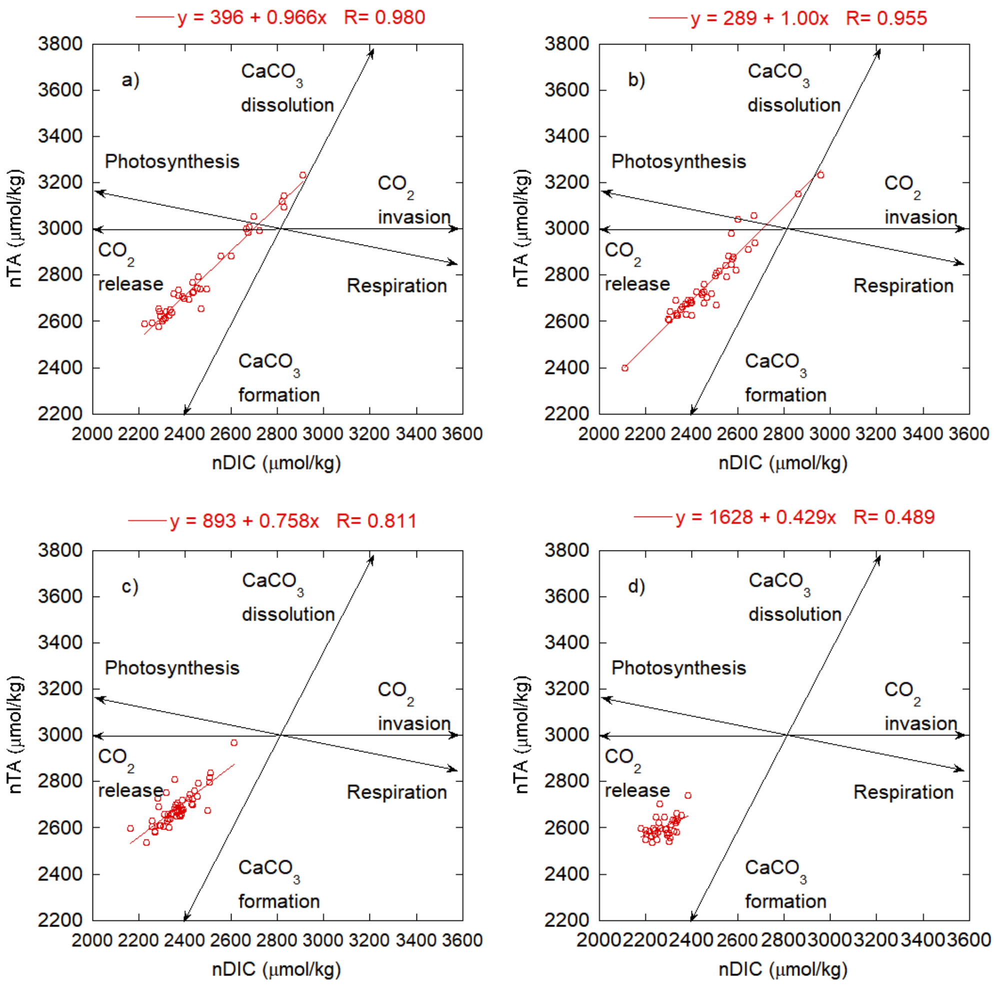

Figure 11. Salinity normalized Total alkalinity (nTA) (µmol/kg) and Dissolved Inorganic Carbon (nDIC) (µmol/kg) plots at STB site (depth: 1 m) during four different periods: a) November-December- January (NDJ), b) February, March April (FMA), c) May-June-July (MJJ), d) August-

September-October (ASO).For each period, regression line equation and correlation coefficients(R) are reported in red on the top of the figures. The black vectors are represented following the stoichiometric ratios of the main biogeochemical processes in order to visualize the dominant processes driving the CO_2 system.

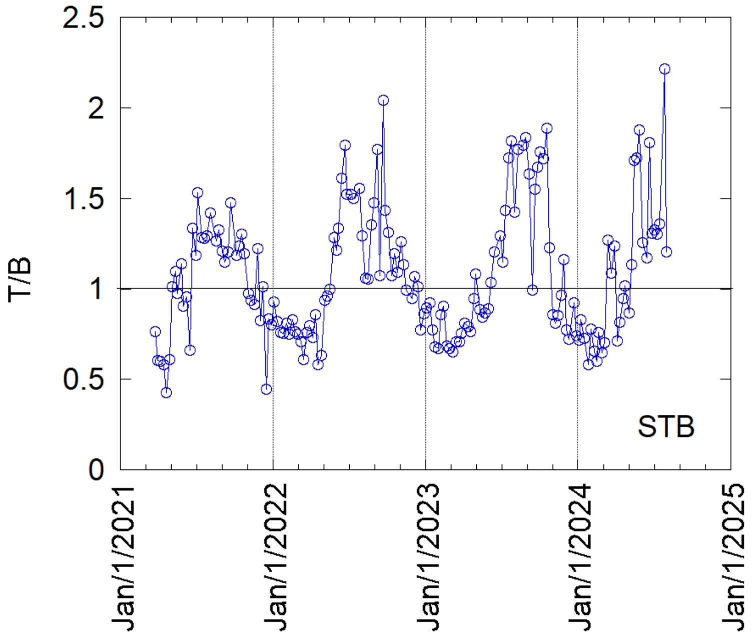

Fig. 12. Temporal patterns of Thermic pCO_2 /Biogenic pCO_2 (T/B) in STB site.

The T/B ratios (i.e., T= thermic, B= biogenic pCO_2) through time revealed that in winter and spring (from November to April) the biogenic processes were dominant, thus CO_2 is removed from seawater by calcifying and photosynthetic processes, leading to the minimum of pCO_2 in surface seawater. Conversely, from May to October, the dominant processes affecting pCO_2 were thermic when pCO_2 were the highest in surface seawater (Fig. 12).

4. Discussion

Ligurian basin has a valuable role observing climate changes of the Mediterranean water masses (Prieur et al., 2020). Given the paucity of information available for the coastal areas of the Ligurian Sea, the multidisciplinary and integrated high-resolution Smart Bay S. Teresa observatory of the Gulf of La Spezia provides valuable insights: it is a hotspot in revealing interesting patterns and variabilities both climate and ecosystem driven.

Anthropogenic climate change is causing deep modifications within the natural systems, including those from the ocean, with consequences on marine ecosystems and communities (Bindoff et al., 2022). The increase of approximately 0.7 °C in average global surface temperature on Earth during the last century has been confirmed by our data showing an average increase of 0.045 °C per year over the 40-year analysis period in agreement with increasing temperature ranges by Darmaraki et al.

(2019). The clear warming trend in the coastal waters of the Gulf of La Spezia, according to the global climate change scenarios caused the increase of extreme warming events, specifically Marine Heatwaves (MHWs), which were documented in the area during 2022-2023 Darmaraki et al., 2019; Oliver et al., 2018). The highest incidence was recorded during summer months, with the longest MHW (21 days) occurring in July 2023, with a maximum thermal anomaly of +3.6 °C compared with daily climatology, highlighting the intensification of these phenomena in recent years (Capotondi et al., 2024; Martìnez et al., 2023; Tejedor et al., 2024).

High seawater temperatures, particularly during MHW events, are deeply affecting marine ecosystems and especially calcifying organisms in the area (Marchini et al., 2019, Ragazzola et al., 2021). The absence of MHW events in 2021, followed by four events in 2022 and others in 2023, suggested an acceleration in the frequency of these phenomena, consistent with what has been reported for other areas of the Mediterranean and responsible for mass mortality events affecting ecosystems (Garrabou et al., 2022). Thus, high-resolution monitoring, observational networks, methodological approaches, forecast models, and artificial intelligence represent key tools for detecting anomalies such as MHW and their effects at regional level (Barriopedro et al., 2023).

The global ocean has been acting as a CO_2 sink by absorbing approximately 25% of annual atmospheric anthropogenic carbon emissions, thus leading to a decrease of ocean pH (i.e., ocean acidification) and an alteration to the ocean carbonate system (Bindoff et al., 2022). Most of the studies on the Mediterranean carbonate system have been conducted on samples collected along zonal transects at the basin scale (Alvarez et al., 2014) or generally indirectly estimated (Schneider et al., 2010; Wimart-Rousseau et al., 2021). Our high-resolution monitoring in a coastal area allowed us to detect weekly and monthly changes in the carbonate system, thus detecting the influence on the environment and ecosystems affected by the ongoing climate change.

The analysis of the carbonate system in the Gulf of La Spezia revealed a favorable environment for calcifying organisms, with saturation values of calcite (Ω_{Ca}) and aragonite (Ω_{Ar}) always above 3, well above the critical threshold for calcium carbonate dissolution. The highest values of Ω_{Ca} (5.5) and Ω_{Ar} (3.6) were recorded at Mussel Aquaculture Buoy (MAB) (depth: 5m) outside the harbour and at Tino Island (TI) (depths: 1m) in the Regional Park, respectively, indicating that seawater biogeochemical conditions promoting calcification processes. Such sites host mollusk farming but also corraligenous habitats with significant in size (i.e., square meters) bioconstructional calcifying ecosystems (Cocito and Sgorbini, 2014; 2012; Nannini et al., 2015; Ragazzola et al., 2021).

Hydrodynamic data showed a clear mitigating effect of the dam on water circulation in the stations within the Gulf of La Spezia. The reduction of the scalar mean current module, from the external to the internal side of the dam, by a factor of about 2 proved the effectiveness of this structure in modifying the local hydrodynamic regime. The directional distribution of currents, with approximately 40% of values distributed along the N-NE-E directions outside the dam, and prevalence along the NE-E and SW-W axes inside, confirmed the structural influence of the dam in channeling marine currents. The observed correlation between the distribution of external currents and the predominant S-SW winds (Bordone, 2019) suggests an important role of local atmospheric forcings on the surface circulation of waters.

Mediterranean evaporation is responsible for higher values of Total Alkalinity (TA) and Salinity (S) compared to those of the Atlantic water entering the Mediterranean Sea (Jiang et al., 2014) and the relationship between these two variables is determined by inputs from rivers and the Black Sea, which are high in TA (Copin-Montegut and Avril, 1993;Schneider et al, 2007). Long-term data series from the western Ligurian Sea revealed a marked seasonality of the carbonate system: TA ranged from 2500 µmol/kg to 2600 µmol/kg, mimicking S_P and showing the lowest values on coastal site (Coppola et al., 2020).

The mean TA values recorded for the area were in the range of those of the west Mediterranean and Tyrrhenian Sea (Alvarez et al., 2014; Fajar et al., 2015) but lower than those measured in the Adriatic Sea (Urbini et al., 2020). Within the studied system, the carbonate environment was not significantly altered by low salinity events (<34) that occurred at all stations at 1 m depth at the end of 2022, demonstrating a stability of the system despite the freshwater inputs (i.e., rain and riverine inputs). Also, the relationship between TA and DIC highlighted the balance between $CaCO_3$ formation processes and CO_2 release, emphasizing the water's ability to capture atmospheric CO_2 and precipitate $CaCO_3$. Calcification processes were dominant over photosynthetic activities across sites, with TA vs DIC slopes ranging from 0.472 for STB to 0.321 for MAB, suggesting a primary role of calcifying organisms in regulating the local carbon cycle (Van Cappellen, 2003).

The high-resolution monitoring conducted at Santa Teresa Bay (STB) revealed distinct temporal patterns in biogeochemical processes. During winter - early spring (November-April), we observed a reduction in pCO_2 and an increase in O_2, accompanied by an increase in $CaCO_3$ formation (nTA *vs* nDIC ratio ≈ 1), suggesting skeleton/shell building activity by calcifying organisms was the driver (Cohen and McConnaughey, 2003). Whereas, the following periods, May-July and August-October, were characterized by minimum O_2 and nutrients and maximum pCO_2, suggesting a progressive prevalence of respiration processes over photosynthetic activities (slope =0.758 and slope=0.429, respectively).

The thermic pCO_2/biogenic pCO_2 proved that biogenic processes during winter and spring (November-April) drove the atmospheric CO_2 removal from seawater through calcification and photosynthesis processes. During this period, pCO_2 concentration in seawater was generally lower than that in the atmosphere (Urbini et al., 2020), thus favoring the CO_2 fluxes from the atmosphere to the sea. Conversely, from May to October the thermic processes (i.e., non-biologically regulated) were dominant, thus pCO_2 concentrations were higher within surface waters that those in the atmosphere, favoring CO_2 fluxes from the sea to the atmosphere.

In addition, the increasing frequency of MHW in summer in the area is exacerbating this process, further reducing the mitigating effect of the ocean. Although the overall results suggest that coastal ecosystems in the Gulf of La Spezia are already experiencing the effects of climate change (Marchini et al., 2019; Ragazzola et al., 2021), the richness of the carbonate system and biochemical fluxes suggested a still favorable environment for calcifying organisms. This is also highlighted by the response of the carbonate system to low salinity events, and the dominance of calcification processes within the area, especially at the investigated sited (1-16 m of depth) rich in calcifying ecosystems (e.g., mussel beds, oysters, bryozoans, coralline algae). However, the expected increase in temperature and frequency of MHWs (Darmaraki et al., 2019), together with water circulation conditions (e.g., presence of dam poses the adaptive capacity of local calcifiers at risk in the next future), with cascading effects on biodiversity and coastal ecosystem functioning.

High-resolution Smart Bay S. Teresa observatory (i.e., high frequency of data acquisition and subsequent validation) confirmed the importance of big data acquisition in marine realm for understanding real-time changes at local scale, mutual influence among marine environment, atmosphere and biological systems in the ocean and how these components can influence each other under the ongoing climate change. Even though limited to a local scale, the described processes confirmed basin dynamics (i.e., Ligurian Sea) and global trends, highlighting how at the local level, marine ecosystems, specifically calcifiers, are contributing to local carbon budget, even though specific studies on carbon fluxes on local ecosystems will be needed. High-resolution and high-quality data from marine systems are necessary to understand the complexity of the occurring processes and especially for the conservation and protection of key ecosystems, fundamental elements in ecosystem-based management strategies to contrast climate change.

5. Conclusions and Perspectives

This study reveals critical dynamics in the Gulf of La Spezia's carbonate reef environment under accelerating climate change. Four decades of temperature data confirm a relentless warming trend of 0.045°C ± 0.003 °C per year, with Marine Heatwaves intensifying dramatically during 2022-2023. These thermal stress events now threaten calcifying organisms with unprecedented frequency, signaling a dangerous acceleration in climate impacts.

The presence of the dam fundamentally alters local hydrodynamics, reducing current velocity by 50% and creating modified flow patterns that may either buffer or amplify climate effects on carbonate systems. This anthropogenic modification introduces critical uncertainty into ecosystem responses, demanding immediate scientific attention to understand whether human infrastructure helps or hinders reef resilience.

Despite rising temperatures and pCO_2 levels, the carbonate system currently maintains favourable conditions for calcification, with calcite and aragonite saturation states remaining above dissolution thresholds. This apparent resilience supports active reef development, yet the favourable window may be closing rapidly as thermal stress intensifies. The system exhibits clear seasonal patterns, with winter-spring calcification dominance transitioning to summer-autumn photosynthetic control, enabling the carbonate environment to function as a seasonal carbon sink during cooler months.

However, the increasing frequency of Marine Heatwaves represents a critical warning. While calcifying organisms currently withstand short-term perturbations, the ecosystem approaches a tipping point where rapid collapse could replace gradual adaptation. The Smart Bay Santa Teresa Observatory exemplifies why continuous, integrated coastal monitoring has become an essential infrastructure rather than optional research. Only real-time, long-term datasets can distinguish natural variability from anthropogenic changes, enabling evidence-based policy decisions and timely ecosystem protection measures.

The convergence of global warming, local hydrodynamic alterations, and seasonal biogeochemical processes creates a complex system approaching critical thresholds. Understanding organism-level responses to multiple stressors, quantifying hydrodynamic-climate interactions, and connecting biogeochemical patterns to ecological responses are now essential for predicting and potentially preventing ecosystem collapse. Integrated monitoring networks represent our most powerful tool for coastal ecosystem survival in an era of accelerating climate change.

CrediT authorship contribution statement

C.Lombardi, T. Ciuffardi, G. Raiteri, S. Becagli: Conceptualization, Supervision, Writing – original draft, Writing – review & editing, T. Ciuffardi, G. Raiteri, S. Becagli, A. Bordone, P. Gjanci, C. Petrioli, D. Spaccini, M. Magaldi, A. Peirano: Formal analysis, Data curation, Methodology, Investigation, Writing – review & editing. F. Piccolin, M. Abbate, I Rossetti, E. Gabrielli: Methodology, Data acquisition, Writing – review & editing.

Declaration of competing interest

None.

Data availability

All data are made publicly available through https://www.seanoe.org (last access: 11 April 2025). The registered database DOI is https://doi.org/10.17882/105897 (Bordone et al., 2025).

The adopted methodology about settings, data records and quality control procedures ensure compliance and consistency of the dataset. The dataset presented conclude in 2024 but monitoring activities are still in progress and future data collected by these stations will be added to an updated version of the repository as advancing of the data collection to convey the progress of oceanographic observations to the scientific community.

Acknowledgements

Real time data through IoUT system have been collected thank to "GREEN SEASTAR" project, a pilot collaboration between Smart Bay S. Teresa (https://smartbaysteresa.com) and WSense R&D. The maintenance of fixed stations over time was possible also thanks to the support of Gruppo Operativo Subacqueo- Comando

Subacquei ed Incursori della Marina Militare and Cooperativa Mitilicoltori Associati. We thank WSense R&D team members who collectively contributed to the design and implementation of the in situ IoUT monitoring network whose design was partially funded by the EASME SEASTAR project.

References

Álvarez, M., Sanleón-Bartolomé, H., Tanhua, T., Mintrop, L., Luchetta, A., Cantoni, C., 2014. The CO2 system in the Mediterranean Sea: a basin wide perspective. Ocean Science, 10, 69–92. https://doi.org/10.5194/os-10-69-2014

Aracri, S., 2019. The seasonal and interannual variability of the Ligurian Sea. University of Southampton, Doctoral Thesis, 1-180.

Barriopedro, D., Garcia-Herrera, R., Ordonez, C., Miralles, D.G., Salcedo-Sanz, S., 2023. Heat waves: Physical understanding and scientific challenges. Reviews of Geophysics, 61, e2022RG000780. https://doi.org/10.1029/2022RG000780

Bindoff, N.L., Cheung, W.W.L., Kairo, J.G., Arístegui, J., Guinder, V.A., Hallberg, R., Hilmi, N., Jiao, N., Karim, M.S., Levin, L., O'Donoghue, S., Purca, S.R., Rinkevich, B., Suga, T., Tagliabue, A., Wimart-Rousseau, C., Wagener, T., Álvarez, M., Moutin, T., Fourrier, M., Coppola, L., et al., 2021. Seasonal and Interannual Variability of the CO2 System in the Eastern Mediterranean Sea: a Case Study in the North Western Levantine Basin. Frontiers in Marine Science, 8, 649246. https://doi.org/10.3389/fmars.2021.649246

Bordone, A., 2019. Dati meterologici acquisiti dalla stazione ENEA di S. Teresa (SP). Rapporto annuale 2018 e comparazione con dati climatologici. Rapporto tecnico RT/2019/5/ENEA, ENEA, Roma.

Borges, A.V., Djenidi, S., Lacroix, G., Théate, J., Delille, B., Frankignoulle, M., 2003. Atmospheric CO2 flux from mangrove surrounding waters. Geophysical Research Letters, 30, 1558. https://doi.org/10.1029/2003GL017143

Bosse, A., Testor, P., Mortier, L., Prieur, L., Taillandier, V., d'Ortenzio, F., Coppola, L., 2015. Spreading of Levantine Intermediate Waters by submesoscale coherent vortices in the northwestern Mediterranean Sea as observed with gliders. Journal of Geophysical Research: Oceans, 120, 1599–1622. https://doi.org/10.1002/2014JC010263

Bramanti, L., Benedetti, M.C., Cupido, R., Cocito, S., Priori, C., Erra, F., Iannelli, M., Santangelo, G., 2016. Demography of animal forests: the example of Mediterranean gorgonians. In: Rossi, S. (Ed.), Marine Animal Forests. Springer International Publishing. https://doi.org/10.1007/978-3-319-17001-5_13-1

Bryan, J.R., Riley, J.P., Williams, P.J.L., 1976. A Winkler procedure for making precise measurements of oxygen concentration for productivity and related studies. Journal of Experimental Marine Biology and Ecology, 21(3), 191-197. https://doi.org/10.1016/0022-0981(76)90114-3

Capotondi, A., Rodrigues, R.R., Sen Gupta, A., et al., 2024. A global overview of marine heatwaves in a changing climate. Communications Earth & Environment, 5, 701. https://doi.org/10.1038/s43247-024-01806-9

Ciuffardi, T., Kokki, Z., Berta, M., Locritani, M., Bordone, A., Delbono, I., Borghini, M., Demarte, M., Ivaldi, R., Pannacciulli, F., Vetrano, A., Marini, D., Caprino, G., 2023. Deep water hydrodynamic observations around a cold water coral habitat in a submarine canyon in the eastern Ligurian Sea (Mediterranean Sea). Earth System Science Data, 15, 1933-1946. https://doi.org/10.5194/essd-15-1933-2023

CNRS, 1973. Résultats des campagnes du N.O. Korotneff (1969–1971). GROUPE HYDROKOR, Centre de Recherches Océanographiques de Villefranche-sur-Mer, Université de Paris VI, Vol. 5.

CNRS, 1975. Résultats des campagnes du N.O. Korotneff (1969–1971). GROUPE HYDROKOR, Centre de Recherches Océanographiques de Villefranche-sur-Mer, Université de Paris VI, Vol. 16.

Cocito, S., Sgorbini, S., 2014. Long term trend in substrate occupation by a clonal carbonate bryozoan in a temperate rocky reef in times of thermal anomalies. Marine Biology, 161, 17-27. https://doi.org/10.1007/s00227-013-2313-x

Cohen, A.L., McConnaughey, T.A., 2003. Geochemical Perspective on Coral Mineralization. Reviews in Mineralogy and Geochemistry, 54, 151-182. https://doi.org/10.2113/0540151

Colella, S., Falcini, F., Rinaldi, E., Sammartino, M., Santoleri, R., 2016. Mediterranean Ocean Colour Chlorophyll Trends. PLOS ONE, 11(6), e0155756. https://doi.org/10.1371/journal.pone.0155756

Copin-Montegut, G., Avril, B., 1993. Vertical distribution and temporal variation of dissolved organic carbon in the North-Western Mediterranean Sea. Deep-Sea Research Part I: Oceanographic Research Papers, 40, 1963–1972. https://doi.org/10.1016/0967-0637(93)90041-Z

Coppola, L., Boutin, J., Gattuso, J.-P., Lefevre, D., Metzl, N., 2020. The Carbonate System in the Ligurian Sea. In: Migon, C., Nival, P., Sciandra, A. (Eds.), The Mediterranean Sea in the Era of Global Change 1. Wiley. https://doi.org/10.1002/9781119706960

Cristini, L., Lampitt, R.S., Cardin, V., Delory, E., Haugan, P., O'Neill, N., Petihakis, G., Ruhl, H.A., 2016. Cost and value of multidisciplinary fixed-point ocean observatories. Marine Policy, 71, 138-146. https://doi.org/10.1016/j.marpol.2016.05.029

Darmaraki, S., Somot, S., Sevault, F., Nabat, P., Cabos Navarez, W.D., Cavicchia, L., Djurdjevic, V., Li, L., Sannino, G., Sein, D.V., 2019. Future evolution of marine heatwaves in the Mediterranean Sea. Climate Dynamics, 53, 1371-1392. https://doi.org/10.1007/s00382-019-04661-z

DelValls, T.A., Dickson, A.G., 1998. The pH of buffers based on 2-amino-2-hydroxymethyl-1,3-propanediol ('tris') in synthetic sea water. Deep Sea Research Part I: Oceanographic Research Papers, 45(9), 1541–1554. https://doi.org/10.1016/S0967-0637(98)00019-3

Dickson, A.G., 1990. Standard potential of the reaction – AgCl(S) +1/2H2(g)=Ag(S) + HCl(Aq) and the standard acidity constant of the ion HSO4- in synthetic sea water from 273.15 to 318.15 K. Journal of Chemical Thermodynamics, 22, 113–127. https://doi.org/10.1016/0021-9614(90)90074-Z

Dickson, A.G., Millero, F.J., 1987. A comparison of the equilibrium constants for the dissociation of carbonic acid in seawater media. Deep-Sea Research Part A, 34, 1733–1743. https://doi.org/10.1016/0198-0149(87)90021-5

Dickson, A.G., Riley, J.P., 1979. The estimation of acid dissociation constants in seawater media from potentiometric titrations with strong base. I. The ionic product of water – KW. Marine Chemistry, 7, 89–99. https://doi.org/10.1016/0304-4203(79)90001-X

Dickson, A., Sabine, C., Christian, J.R., 2007. Guide to Best Practices for Ocean CO2 Measurements. PICES Special Publication 3, IOCCP Report No. 8, 1-196.

Durin, G., Coisson, M., Pennecchi, F., Bordone, A., Ciuffardi, T., Raiteri, G., Petrioli, C., 2023. Forecasting oxygen content in seawater. In: Mathematical and Statistical Methods for Metrology (MSMM 2023), Turin, Italy, 30-31 May 2023, pp. 100-101.

European Strategy Forum on Research Infrastructures, 2021. ESFRI Roadmap 2021 - Strategy Report on Research Infrastructures, Part 1. ESFRI Secretariat, Luxembourg, 26 pp. https://doi.org/10.25607/OBP-1861

Fajar, N.M., García-Ibáñez, M.I., SanLeón-Bartolomé, H., Álvarez, M., Pérez, F.F., 2015. Spectrophotometric Measurements of the Carbonate Ion Concentration: Aragonite Saturation States in the Mediterranean Sea and Atlantic Ocean. Environmental Science & Technology, 49, 11679−11687. https://doi.org/10.1021/acs.est.5b03033

Fennel, K., Gehlen, M., Brasseur, P., Brown, C.W., Ciavatta, S., Cossarini, G., et al., 2019. Advancing marine biogeochemical and ecosystem reanalyses and forecasts as tools for monitoring and managing ecosystem health. Frontiers in Marine Science, 6, 89. https://doi.org/10.3389/fmars.2019.00089

Ferri, V., Thomas, S.O., Bordone, A., Raiteri, G., Ciuffardi, T., Lombardi, C., Petrioli, C., Spaccini, D., Gjanci, P., Pennecchi, F., Coisson, M., Durin, G., 2024. A Multi-Stage Model for Dissolved Oxygen Monitoring of Coastal Seawater. 2024 IEEE International Workshop on Metrology for the Sea; Learning to Measure Sea Health Parameters (MetroSea), Portorose, Slovenia, 501-506. https://doi.org/10.1109/MetroSea62823.2024.10765778

Freestone, D., Bjergstrom, K.N., Gjerde, K.M., Halpin, P., Fleming, K.P., Hudson, A., Rogers, A.D., Sapsford, F., Tsontos, V.M., Vazquez-Cuervo, J., Vousden, D., 2024. High seas in the cloud: the role of big data and artificial intelligence in support of high seas governance– The Sargasso Sea pilot. Frontiers in Marine Science, 11, 1427099. https://doi.org/10.3389/fmars.2024.1427099

Friis, K., Körtzinger, A., Wallace, D.W.R., 2003. The salinity normalization of marine inorganic carbon chemistry data. Geophysical Research Letters, 30, 1085. https://doi.org/10.1029/2002GL015898

Garrabou, J., Gomez-Gras, D., Medrano, A., Cerrano, C., Ponti, M., Schlegel, R., Bensoussan, N., Turricchia, E., Sini, M., Gervasi, V., et al., 2022. Marine heatwaves drive recurrent mass mortalities in the Mediterranean Sea. Global Change Biology, 28, 5708-5725. https://doi.org/10.1111/gcb.16301

Gasparini, G.P., Abbate, M., Bordone, A., Cerrati, G., Galli, C., Lazzoni, E., Negri, A., 2009. Circulation and biomass distribution during warm season in the Gulf of La Spezia (north-western Mediterranean). Journal of Marine Systems, 78, S48-S62. https://doi.org/10.1016/j.jmarsys.2009.01.010

Giorgi, F., 2006. Climate change hot-spots. Geophysical Research Letters, 33, L08707. https://doi.org/10.1029/2006GL025734

Goffart, A., Hecq, J.-H., Prieur, L., 1995. Contrôle du phytoplancton du bassin Ligure par le front liguro-provençal (secteur Corse). Oceanologica Acta, 18, 329–342.

Gostan, J., 1967. Comparaison entre les conditions hydrologiques et climatiques observées dans le Golfe de Gênes pendant les hivers 1962–1963 et 1963–1964. Cahiers Hydrographiques, 19, 391–416.

Grasshoff, K., Ehrhardt, M., Kremling, K., 1983. Methods of Seawater Analysis, 2nd Edition. Verlag Chemie, Weinheim, New York, 1-419.

Hobday, A.J., Alexander, L.V., Perkins, S.E., Smale, D.A., Straub, S.C., Oliver, E.C., Benthuysen, J.A., Burrows, M.T., Donat, M.G., Feng, M., 2016. A hierarchical approach to defining marine heatwaves. Progress in Oceanography, 141, 227–238. https://doi.org/10.1016/j.pocean.2015.12.014

Hurd, C.L., Cornwall, C.E., Currie, K., Hepburn, C.D., McGraw, C., Hunter, K.A., Boyd, P., 2011. Metabolically induced pH fluctuations by some calcifiers exceed projected 22nd century ocean acidification: a mechanism for different susceptibility? Global Change Biology, 17, 3254–3262. https://doi.org/10.1111/j.1365-2486.2011.02473.x

Janzen, C., Murphy, D., Larson, N., 2007. Getting more mileage out of dissolved oxygen sensors in long-term moored applications. OCEANS 2007, IEEE. https://doi.org/10.1109/OCEANS.2007.4449398

Jiang, Z.-P., Tyrrell, T., Hydes, D.J., Dai, M., Hartman, S.E., 2014. Variability of alkalinity and the alkalinity-salinity relationship in the tropical and subtropical surface ocean. Global Biogeochemical Cycles, 28(7), 729-742. https://doi.org/10.1002/2013GB004678

Krumins, V., Gehlen, M., Arndt, S., Van Cappellen, P., Regnier, P., 2013. Dissolved inorganic carbon and alkalinity fluxes from coastal marine sediments: model estimates for different shelf environments and sensitivity to global change. Biogeosciences, 10, 371–398. https://doi.org/10.5194/bg-10-371-2013

Langdon, C., 2010. Determination of Dissolved Oxygen in Seawater by Winkler Titration using Amperometric Technique. In: Hood, E.M., Sabine, C.L., Sloyan, B.M. (Eds.), The GO-SHIP Repeat Hydrography Manual: A Collection of Expert Reports and Guidelines, Version 1. IOCCP Report Number 14, ICPO Publication Series Number 134, 1-18. https://doi.org/10.25607/OBP-1350

Lombardi, C., Taylor, P.D., Cocito, S., 2020. Bryozoans: The 'Forgotten' Bioconstructors. In: Rossi, S., Bramanti, L. (Eds.), Perspectives on the Marine Animal Forests of the World. Springer, Cham. https://doi.org/10.1007/978-3-030-57054-5_7

Ma, Q., Durin, G., Pennecchi, F., Lombardi, C., Petrioli, C., 2022. Bayesian Machine Learning and variational inference for on-site sensor calibration in Smart Bay Santa Teresa seawater monitoring. In: MATHMET 2022, Paris, France, 2-4 November 2022.

Marchini, A., Ragazzola, F., Vasapollo, C., Castelli, A., Cerrati, G., Gazzola, F., Jiang, C., Langeneck, J., Manauzzi, M.C., Musco, L., Nannini, M., Zekonyte, J., Lombardi, C., 2019. Intertidal Mediterranean Coralline Algae Habitat Is Expecting a Shift Toward a Reduced Growth and a Simplified Associated Fauna Under Climate Change. Frontiers in Marine Science, 6, 106. https://doi.org/10.3389/fmars.2019.00106

Martínez, J., Leonelli, F.E., García-Ladona, E., Garrabou, J., Kersting, D.K., Bensoussan, N., Pisano, A., 2023. Evolution of marine heatwaves in warming seas: the Mediterranean Sea case study. Frontiers in Marine Science, 10, 1193164. https://doi.org/10.3389/fmars.2023.1193164

Marullo, S., Serva, F., Iacono, R., Napolitano, E., di Sarra, A., Meloni, D., Monteleone, F., Sferlazzo, D., De Silvestri, L., de Toma, V., Pisano, A., Bellacicco, M., Landolfi, A., Organelli, E., Yang, C., Santoleri, R., 2023. Record-breaking persistence of the 2022/23 marine heatwave in the Mediterranean Sea. Environmental Research Letters, 18, 114041. https://doi.org/10.1088/1748-9326/ad02ae

Mehrbach, C., Culberson, C.H., Hawley, J.E., Pytkowicz, R.M., 1973. Measurements of the apparent dissociation constants of carbonic acid in seawater at atmospheric pressure. Limnology and Oceanography, 18, 897–907. https://doi.org/10.4319/lo.1973.18.6.0897

Merchant, C.J., Embury, O., Bulgin, C.E., Block, T., Corlett, G.K., Fiedler, E., Good, S.A., Mittaz, J., Rayner, N.A., Berry, D., Eastwood, S., Taylor, M., Tsushima, Y., Waterfall, A., Wilson, R., Donlon, C., 2019. Satellite-based time-series of sea-surface temperature since 1981 for climate applications. Scientific Data, 6, 223. https://doi.org/10.1038/s41597-019-0236-x

Micheli, F., Halpern, B.S., Walbridge, S., Ciriaco, S., Ferretti, F., Fraschetti, S., Lewison, R., Nykjaer, L., Rosenberg, A.A., 2013. Cumulative human impacts on Mediterranean and Black Sea marine ecosystems: assessing current pressures and opportunities. PLOS ONE, 8, e79889. https://doi.org/10.1371/journal.pone.0079889

Migon, C., Nival, P., Sciandra, A., 2020. The Mediterranean Sea in the Era of Global Change 2. Thirty years of Multidisciplinary Study of the Ligurian Sea. ISTE Ltd and John Wiley & Sons, Inc. https://doi.org/10.1002/9781119704782

Millero, F.J., Lee, K., Roche, M., 1998. Distribution of alkalinity in the surface waters of the major oceans. Marine Chemistry, 60, 111–130. https://doi.org/10.1016/S0304-4203(97)00084-4

Millot, C., Taupier-Letage, I., 2005. Circulation in the Mediterranean Sea. In: Saliot, A. (Ed.), The Mediterranean Sea. Springer, Berlin, Heidelberg. https://doi.org/10.1007/b107143

Nannini, M., De Marchi, L., Lombardi, C., Ragazzola, F., 2015. Effects of thermal stress on the growth of an intertidal population of Ellisolandia elongata (Rhodophyta) from N-W Mediterranean Sea. Marine Environmental Research, 112, 11-19. https://doi.org/10.1016/j.marenvres.2015.05.005

Palmiéri, J., Orr, J.C., Dutay, J.C., Béranger, K., Schneider, A., Beuvier, J., Somot, S., 2015. Simulated anthropogenic CO2 storage and acidification of the Mediterranean Sea. Biogeosciences, 12, 781–802. https://doi.org/10.5194/bg-12-781-2015

Paulsen, M.L., Dickson, A.G., 2020. Preparation of 2-amino-2-hydroxymethyl-1,3-propanediol (TRIS) pHT buffers in synthetic seawater. Limnology and Oceanography: Methods, 18, 504-515. https://doi.org/10.1002/lom3.10380

Peirano, A., Cocito, S., Banfi, V., Cupido, R., Damasso, V., Farina, G., Lombardi, C., Mauro, R., Morri, C., Roncarolo, I., Saldaña, S., Savini, D., Sgorbini, S., Silvestri, C., Stoppelli, N., Torricelli, L., Bianchi, C.N., 2011. Phenology of the Mediterranean seagrass Posidonia oceanica (L.) Delile: Medium and long term cycles and climate inferences. Aquatic Botany, 94(2), 77-92. https://doi.org/10.1016/j.aquabot.2010.11.007

Pinardi, N., Zavatarelli, M., Adani, M., Coppini, G., Fratianni, C., Oddo, P., Simoncelli, S., Tonani, M., Lyubartsev, V., Dobricic, S., Bonaduce, A., 2015. Mediterranean Sea large-scale low-frequency ocean variability and water mass formation rates from 1987 to 2007: a retrospective analysis. Progress in Oceanography, 132, 318–332. https://doi.org/10.1016/j.pocean.2013.11.003

Prieur, L., D'Ortenzio, F., Taillandier, V., Testor, P., 2020. Physical oceanography of the Ligurian Sea. In: Migon, C., Nival, P., Sciandra, A. (Eds.), The Mediterranean Sea in the Era of Global Change 1. Wiley. https://doi.org/10.1002/9781119706960.ch3

Ragazzola, F., Kolzenburg, R., Adani, M., Bordone, A., Cantoni, C., Cerrati, G., Ciuffardi, T., Cocito, S., Luchetta, A., Montagna, P., Nannini, M., Page, D., Peirano, A., Raiteri, G., Lombardi, C., 2021. Carbonate chemistry and temperature dynamics in an algae dominated habitat. Regional Studies in Marine Science, 44, 101770. https://doi.org/10.1016/j.rsma.2021.101770

Ruhl, H.A., André, M., Beranzoli, L., Çağatay, M.N., Colaço, A., Cannat, M., Dañobeitia, J.J., Favali, P., Géli, L., Gillooly, M., Greinert, J., Hall, P.O.J., Huber, R., Karstensen, J., Lampitt, R.S., Larkin, K.E., Lykousis, V., Mienert, J., Miranda, J.M., Person, R., Priede, I.G., Puillat, I., Thomsen, L., Waldmann, C., 2011. Societal need for improved understanding of climate change, anthropogenic impacts, and geo-hazard warning drive development of ocean observatories in European Seas. Progress in Oceanography, 91, 1-33. https://doi.org/10.1016/j.pocean.2011.05.001

Saderne, V., Baldry, K., Anton, A., Agustí, S., Duarte, C.M., 2019. Characterization of the CO2 system in a coral reef, a seagrass meadow, and a mangrove forest in the central Red Sea. Journal of Geophysical Research: Oceans, 124, 7513–7528. https://doi.org/10.1029/2019JC015266

Saha, K., Zhao, X., Zhang, H.-M., Casey, K.S., Zhang, D., Baker-Yeboah, S., Kilpatrick, K.A., Evans, R.H., Ryan, T., Relph, J.M., 2018. AVHRR Pathfinder version 5.3 level 3 collated (L3C) global 4km sea surface temperature for 1981-Present. NOAA National Centers for Environmental Information Dataset. https://doi.org/10.7289/v52j68xx

Schneider, A., Wallace, D.W.R., Körtzinger, A., 2007. Alkalinity of the Mediterranean Sea. Geophysical Research Letters, 34, L15608. https://doi.org/10.1029/2006GL028842

Schneider, A., Tanhua, T., Körtzinger, A., Wallace, D.W.R., 2010. High anthropogenic carbon content in the eastern Mediterranean. Journal of Geophysical Research, 115, C12050. https://doi.org/10.1029/2010JC006171

Siokou-Frangou, I., Christaki, U., Mazzocchi, M.G., Montresor, M., Ribera d'Alcalá, M., Vaqué, D., et al., 2010. Plankton in the open Mediterranean Sea: a review. Biogeosciences, 7, 1543–1586. https://doi.org/10.5194/bg-7-1543-2010

Sippo, J.Z., Maher, D.T., Tait, D.R., Holloway, C., Santos, I.R., 2016. Are mangroves drivers or buffers of coastal acidification? Insights from alkalinity and dissolved inorganic carbon export estimates across a latitudinal transect. Global Biogeochemical Cycles, 30, 753–766. https://doi.org/10.1002/2015GB005324

Takahashi, T., Sutherland, S.C., Sweeney, C., Poisson, A., Metzl, N., Tilbrook, B., 2002. Global sea–air CO2 flux based on climatological surface ocean pCO2, and seasonal biological and temperature effects. Deep-Sea Research Part II, 49, 1601–1622. https://doi.org/10.1016/S0967-0645(02)00003-6

Tejedor, E., Benito, G., Serrano-Notivoli, R., et al., 2024. Recent heatwaves as a prelude to climate extremes in the western Mediterranean region. npj Climate and Atmospheric Science, 7, 218. https://doi.org/10.1038/s41612-024-00771-6

Uchida, H., Johnson, G.C., McTaggart, K.E., 2010. CTD Oxygen Sensor Calibration Procedures. In: Hood, E.M., Sabine, C.L., Sloyan, B.M. (Eds.), The GO-SHIP Repeat Hydrography Manual: A Collection of Expert Reports and Guidelines, Version 1. IOCCP Report Number 14, ICPO Publication Series Number 134, 17 pp. https://doi.org/10.25607/OBP-1344

United Nations, 2015. Transforming our world: The 2030 Agenda for Sustainable Development. Resolution adopted by the General Assembly on 25 September 2015, A/RES/70/1.

Uppström, L.R., 1974. The boron/chlorinity ratio of deep-sea water from the Pacific Ocean. Deep Sea Research, 21, 161–162. https://doi.org/10.1016/0011-7471(74)90074-6

Urbini, L., Ingrosso, G., Djakovac, T., Piacentino, S., Giani, M., 2020. Temporal and spatial variability of CO2 system in a riverine influence area of the Mediterranean Sea, the Northern Adriatic. Frontiers in Marine Science, 7, 679. https://doi.org/10.3389/fmars.2020.00679

Van Cappellen, P., 2003. Biomineralization and Global Biogeochemical Cycles. Reviews in Mineralogy and Geochemistry, 54, 357–381. https://doi.org/10.2113/0540357

von Jackowski, A., 2025. Navigating the current landscape of ocean observations: an overview from platform infrastructures to networks related to ocean time series. Frontiers in Marine Science, 11, 1363863. https://doi.org/10.3389/fmars.2024.1363863

Winkler, L.W., 1888. The determination of dissolved oxygen. Berichte der Deutschen Chemischen Gesellschaft, 21, 2843–2846. https://doi.org/10.1002/cber.188802102122

Wolfe, K., Nguyen, H.D., Davey, M., Byrne, M., 2020. Characterizing biogeochemical fluctuations in a world of extremes: a synthesis for temperate intertidal habitats in the face of global change. Global Change Biology, 26, 3858–3879. https://doi.org/10.1111/gcb.15103

Zeebe, R.E., Wolf-Gladrow, D., 2001. CO2 in Seawater: Equilibrium, Kinetics, Isotopes. Elsevier Oceanography Series, Amsterdam.lliamson, P., 2022. Changing Ocean, Marine Ecosystems, and Dependent Communities. In: Pörtner, H.O., Roberts, D.C., Masson-Delmotte, V., Zhai, P., Tignor, M., Poloczanska, E., Mintenbeck, K., Alegría, A., Nicolai, M., Okem, A., Petzold, J., Rama, B., Weyer, N.M. (Eds.), The Ocean and Cryosphere in a Changing Climate Special Report of the Intergovernmental Panel on Climate Change. Cambridge University Press, 5, 447-587. https://doi.org/10.1017/9781009157964